Apèndix A

Llista d'acrònims

AEDOS	Advanced Earth Observing Satellite
AOT	Aerosol Optical Thickness
ASCII	American Standard Code for Information Interchange
ATMOS	Atmospheric Trace MOlecule Spectroscopy
CIE	Commission Internationale de l'Eclairage
CLAES	Cryogenic Limb Array Etalon Spectrometer
CMF	Cloud Modification Factor
CFC	Clor-Fluor-Carbur
COST	COoperation europeenne dans le domaine de la recherche Scientifique et Technique
DISORT	DIscrete Ordinate Radiative Transfer
DOAS	Differential Optical Absorption Spectroscopy
DWD	Deutscher WetterDienst
ECMWF	European Centre for Medium-range Weather Forecasts
ERS	European Remote Satellites

ESA	European Space Agency
FORTRAN	FORmula TRANslator
FOV	Field Of Vision
FWHM	Full Width at Half Maximum
GME	Global Modell
GOME	Global Ozone Monitoring Experiment
GOMOS	Global Ozone Monitoring by Occultation of Stars
HALOE	Halogen Occultation Experiment
HiRDLS	High Resolution Dynamics Limb Sounder
INM	Instituto Nacional de Meteorología
INTA	Instituto Nacional de Técnica Aerospacial
LIMS	Limb Infrared Monitor of Stratosphere
LOWTRAN	LOW resolution TRANsmission
MBE	Mean Bias Error
MED	Minimum Eritema Dose
MODTRAN	MODerate resolution TRANsmittance
NASA	National Aeronautics and Space Administration
ND(1)	Neutral Density
OS(400/700)	Operating System
POAM	Polar Ozone and Aerosol Measurement
RAF	Radiation Amplification Factor
RMSE	Root Mean Square Error

SAGE	Stratospheric Aerosol and Gas Experiment
SBDART	Santa Barbara DISORT Atmospheric Radiative Transfer
SBUV	Solar Backscatter UltraViolet
SCIAMACHY	Scanning Imaging Absorption SpectroMeter Atmospheric CHartographY
SMARTS	Simple Model for the Atmospheric Radiative Transfer of Sunshine
SMC	Servei Meteorològic de Catalunya
STAR	System for a Transfer of Atmospheric Radiation
TES	Tropospheric Emission Spectrometer
TOMS	Total Ozone Mapping Spectrometer
TUV	Tropospheric Ultraviolet and Visible radiative transfer code
UD	Unitat Dobson
UV	Ultraviolat/da
UVAGOA	Universidad de VAlladolid Grupo Optica Atmosférica
YES	Yankee Environmental Systems

Apèndix B

Paràmetres estadístics utilitzats

Biaix (MBE*; Mean Bias Error*): Serveix per determinar si una variable x té en conjunt uns valors majors o menors que la variable y. Per defecte, quan no s'especifiqui res més, en comparar dues variables x i y, el seu biaix s'haurà calculat fent la resta x - y.

$$MBE = \frac{1}{N}\sum_{i=1}^{N} x_i - y_i \ . \tag{B.1}$$

Error quadràtic mitjà (RMSE; *Root Mean Square Error*): Serveix per determinar les desviacions entre dues variables x i y evitant que es compensin les diferències negatives i positives respecte de la mitjana.

$$RMSE = \sqrt{\frac{1}{N}\sum_{i=1}^{N}(x_i - y_i)^2} \ . \tag{B.2}$$

Tant el biaix com l'error quadràtic mitjà són paràmetres útils a l'hora de caracteritzar les diferències absolutes o relatives entre dues variables. En aquest darrer cas, per calcular-ho s'ha pres per defecte la diferència relativa entre x i y com $\frac{x-y}{x}$, excepte en el cas de comparar models i mesures, assignant sempre com a denominador, la mesura.

Coeficient de correlació (r^2): Serveix per indicar si dues variables x i y estan molt o poc correlacionades.

$$r^2 = \frac{[\sum_{i=1}^{N}(x_i - \overline{x} >)(y_i - \overline{y} >)]^2}{\sum_{i=1}^{N}(x_i - \overline{x} >)^2 \sum_{i=1}^{N}(y_i - \overline{y})^2} \ , \tag{B.3}$$

on $\overline{x}$ i $\overline{y}$ són les mitjanes de les variables x i y i es calculen com:

$$\overline{x} = \frac{1}{N}\sum_{i=1}^{N} x_i \ . \tag{B.4}$$

Apèndix C

Publicacions

C.1 Photochemistry and Photobiology. Vol. preprint, 2005

American Society for Photobiology Journal preprint:N/A–N/A (2005)
DOI: 10.1562/2004-11-25-RA-380

doi: 10.1562/2004-11-25-RA-380
Photochemistry and Photobiology: Vol. preprint, No. preprint.

The UV Index On The Spanish Mediterranean Coast

M. J. Marín,[1] Y. Sola,[2] F. Tena,[1] M.P. Utrillas,[1] E. Campmany,[2] X. de Cabo,[2] J. Lorente,[2] and Jose A. Martínez-Lozano[1]

[1]University of Valencia

[2]University of Barcelona

Received 25 November 2004; revised 8 February 2005; accepted 10 February 2005; published online 21 February 2005

ABSTRACT

An analysis is made of measured ultraviolet erythemal solar radiation (UVER) data recorded during the year 2003 by the networks of the Catalan Weather Service and the Environment Department of Valencia (both on the Spanish Mediterranean coast). Results show a latitudinal variation, at sea level, of 3-4% per degree and an increase with altitude of 10% per km. Based on these data the Ultraviolet Index (UV Index) has been evaluated for the measuring stations. The maximum experimental value of the UV Index was around 9 during the summer, although higher values were recorded at two stations; one at the highest elevation and the other at the lowest latitude. The annual accumulated doses of irradiation on a horizontal plane have been presented as well as the evolution through the year in units of energy, SEDs (Standard Erythemal Doses) and MEDs (Minimum Erythemal Doses) according to different phototypes. Lastly, the UV Index forecast, determined with a multiple- scattering radiative transfer model, has been analysed. Total agreement or only one unit of difference between measured and modelled values was found in 94% of cloud-free cases.

Key words: Ultraviolet erythemal solar radiation, UV Index, UV modelling

INTRODUCTION

In the middle of the 1980's, spurred by public concern following the discovery of the ozone hole in the Southern Hemisphere (1), many atmospheric researchers and medical professionals recognised the need to introduce indices for predicting the doses of ultraviolet radiation incident at ground level. Such indices are aimed at raising public awareness, through the media, of the levels of ultraviolet (UV) radiation incident at ground level and its possible harmful effects. They constitute a simple means of expressing the intensity of UV radiation in relation to its capacity to trigger certain biological processes.

In 1995 the International Commission on Non-Ionizing Radiation Protection (ICNIRP) in collaboration with the WHO (World Health Organization), the WMO (World Meteorological Organization) and the UNEP (United Nations Environmental Program) produced recommendations redefining the ultraviolet radiation index (UV Index) (2). Subsequently the WMO (3) defined the effective erythemal radiation as the spectral solar irradiance biologically weighted by the action spectrum recommended by the Comission Internationale de l'Eclarage, CIE, (4,5) on a horizontal surface at ground level. Quantitatively, the UV Index is determined from the integrated erythemally weighted radiation (UVER) over all wavelengths up to 400 nm (expressed in Wm^{-2}) multiplied by 40. It is rounded to the nearest whole number. For sloping surfaces, directed toward the Sun, this value could be higher (6).

Forecasting of the UV Index may be done by using many different radiative transfer models, although the COST-713 Action of the European Commission recommends the use of multiple scattering models for this since these show better agreement between

simulations (7). To validate the accuracy of UV Index forecasts, it is necessary to have accurate and precise UVER measurements. Moreover, such experimental UVER values are also useful for developing a UV radiation climatology and establishing geographical and seasonal distributions of UV exposure; information which is useful in many areas including human health (8,9).

In Spain, the National Institute of Meteorology (INM) installed a measurement network, based on broad band radiometers, at the beginning of 1999. At present it consists of 16 UVB pyranometers and 6 Brewer spectrophotometers to also determine the total ozone column (10,11). At the same time, many autonomous regions, which in Spain currently have responsibility for many issues including the environment and tourism, have developed their own erythemal radiation measurement networks. These regional networks complement the state network with a higher spatial resolution. Two such networks are found in the regions of Catalonia and Valencia which occupy a large stretch in the Spanish Mediterranean coast (see Fig. 1) and receive many of the 42 millions of tourists that every year visit Spain, making the regions one of the most touristic areas of Europe.

This paper presents an analysis of the UV Index and corresponding measurements for both regions for 2003. A comparative study has been carried out between experimental and modelled values using multiple scattering radiative transfer models. This analysis completes a previous paper for the two main cities of these regions, Barcelona and Valencia (12).

MATERIAL AND METHODS

a) Measurement networks

The UV Index measurement network in Catalonia was established in the middle of 2000. It was designed by the Department of Astronomy and Meteorology of the University of Barcelona. The network consists of 4 stations; three located on the coast and the other inland at an altitude of 1400 m above sea level. The location of these is shown in Fig. 1. Similarly, the Environment Department of the Regional Government of Valencia established a UVB radiation measurement network with 5 stations. Designed by the Solar Radiation Group of the University of Valencia the network consists of four stations on the coast and another inland at 1300 m altitude. The location of these stations is also shown in Fig. 1. Table I gives the stations' locations and elevations above mean sea level. The higher density of stations in coastal locations is justified as much by the high stable population as by the importance of the tourist destinations. The inland stations are useful for studying continental and altitude effects.

The sensors installed in the Valencian network are UVB-1 pyranometers of the YES Company (Yankee Environmental Systems, Turners Falls, MA 01376 USA). The national UV network of Spain uses these same instruments (10). The sensors installed in Catalonia are 501A UV biometers of the Solar Light Company (Glenside, PA 19038 USA). All these radiometers are broad-band (280-330 nm) Robertson-Berger-type (RB) radiometers. The RB meter was designed to measure the erythemal dose of the solar radiation by means of a fluorescent phosphor that converts the UVB light to visible light that is then measured by a solid state photodetector. The response of these instruments

is similar to the spectral response of human skin to UV radiation, although these broad-band instruments do not exactly match the weighting function. A methodology to determine how to correct the outputted values with respect to total ozone and solar zenith angle is given by Lantz et al. (13).

These sensors are designed to be stable for long periods of time and for field experiments and do not require continuous attention. In each measurement station, the instrument has been installed with an uninterrupted and stabilized battery, a pole with platform to mount the sensor and a communication antenna, and a protected enclosure with an electrical installation. The data acquisition and transmission include communication software and protocols and a GSM communication system.

Although the radiometers are provided calibrated by the manufacturer, they are re-calibrated periodically, approximately once a year. The calibration is carried out by two different procedures, firstly by comparison with a high resolution spectroradiometer and the secondly by comparison with a standard radiometer with similar characteristics. In the first procedure two spectroradiometers, Bentham (Reading RG2 0NH England) DM 300 and Optronic (Orlando, FL 32811 USA) OL-754, are used for Catalonia and Valencia, respectively. The second method, known as intercomparison, is usually used in UVB networks (14-16). The network radiometers are calibrated by comparing their responses with a similar radiometer, called the standard which has been calibrated previously by a reference lamp or a precision spectroradiometer. For the intercomparison, all the instruments are placed on a horizontal surface, 1.5 m above the ground and separated 40 cm from each other in order to avoid shadows. The

measurements are made simultaneously during two or three days, with fixed specifications such as sample time, scale factor, temperature stabilization, etc.

The radiometers, in standard operating mode, measure UVER (Wm^{-2}) every second. From these values the integrated irradiance values are obtained for the desired time interval, in this case one minute. These data constitute the primary database for determining the experimental UV Index following the recommendations of WHO/WMO/ICNIRP/UNEP (2,8) and COST 713 Action (17). Later, from this primary database, and once screened, the 10 minute means are determined, so that the secondary data base consists of 10 minute UVER measurements which are used to calculate the UV Index and its daily evolution. Generally the maximum corresponds with the solar noon.

b) UV Index forecast

The UV Index forecast is calculated by multiple scattering radiative transfer models that usually provide this value directly as an output product (7). The essential input data are date and time, geographical coordinate system, altitude above sea level and vertical ozone column. Results from various models have been analysed and compared before finally the SBDART algorithms (2.0 and 2.3 versions) were implemented. SBDART is the acronym of "Santa Barbara DISORT Atmospheric Radiative Transfer", and was developed by Richiazzi *et al.* (18). This program, written in FORTRAN, is designed for the analysis of a wide variety of radiative transfer problems across the atmosphere considering satellite data and energy balance studies in the atmosphere. It is available for free from various web sites (19, 20).

In the SBDART model, the radiative transfer equation is solved numerically integrating with the DISORT method (DIScreet Ordinate Radiative Transfer). This provides a stable algorithm to solve the radiative transfer equations in a vertically non-homogeneous plane-parallel atmosphere, using as many as 40 layers and 16 zenital and azimutal angles. Once SBDART has been executed, the UV Index is calculated. This calculus has been automated by a FORTRAN program which calculates the index in various stages: a) spectral erythemal irradiance; b) integrated erythemal irradiance; and c) UV Index.

The model is implemented for clear days forecast for sea level, using as ozone column input the values supplied by TOMS (21). The clouds and altitude corrections in the UV Index are made at a later stage, once the prediction for clear days has been made, according to the methodology suggested by COST 713 (17):

$$UVI = UVI_0 \cdot CMF \cdot (1 + 0.08 \cdot \Delta H)$$

where UVI_0 is cloud-free sky UV Index, CMF is cloud modification factor (a non-dimensional number between 0 and 1, see Table II) and ΔH is the elevation of the surface above sea level in km.

Every day the radiation groups of the Universities of Barcelona and Valencia make 36 hour UV Index forecasts corresponding to solar noon. The broadcasting of this forecast is achieved through the Catalan Weather Service web site (http://www.meteocat.com) and the Valencian Environment Office site (http://www.cma.gva.es/cidam/emedio/uv/).

RESULTS AND DISCUSION

a) Experimental values of the UV Index

In Fig. 2 (a-i) the 2003 annual evolution of the daily values of UVER corresponding to solar noon is shown for each station of the measurement networks. Likewise, Table III shows monthly means of cloud-free daily values of UVER for each station.

In view of these tables, there are some observations about the influence of height and latitude in the UVER can be made. As for latitudinal effect, the analysis of the values of 2° distant stations, but at the same altitude above sea level, Roses (42° 16' 16" N), Prat de Cabanes (40° 08' 13" N) and La Mata (38° 00' 30" N), shows an average decrease of 6 % per degree. The altitude effect has been deduced by the comparison between data of Molló and Roses (at similar latitude) and Aras de Olmos and Valencia (0.5° distant in latitude). The first pair of stations shows an increase of 16 % per km; whilst for the second pair the increment is 21 % per km. These results are considerably higher than the estimated by the COST-713 Action (17).

The data have been recalculated employing only values of UVER corresponding to a UV Index equal to or higher than 3 (UVER higher than 0.075 Wm^2). This criterion was chosen because this is the threshold of moderate UV Index and above which protective tools are necessary (3). This level was reached in the months between March and September in Catalonia and from March to October in Valencian Region. The latitudinal effect in this case is 4 %. The altitude effect for Molló and Roses is now of a 10 % per km, and for Aras de Olmos and Valencia the increment is 11% per km. This slight difference could be assumed to be a product of the latitudinal effect which is not

negligible in this case. This percentage fits with the value at noon estimated by the COST-713 Action (17).

In this analysis the possible differences/similarities in site conditions own to albedo (snow, grassy vs. bare ground) and polluted (high aerosol) vs. non-polluted (low aerosol), that could present an additional influence between the high and low elevation sites have not been considered. This is particularly important if there is snow in the mountain stations because the increasing in the albedo could explain the big differences in altitude obtained in the winter season.

The COST-713 Action proposed a UV Index increase of about 8% per km. Frederick (1993, personal communication) found an increase of 6% per km through modelling whereas Blumthaler *et al.* (22) found about 14%-18% per km from measurements on a horizontal surface. The ten percentage points per km found in this study is close to the 8% per km suggested in the equation shown previously to determine the UV Index.

Although it is currently recommended that the UV Index represents the maximum daily value of the UVER, the experimental UV Index was determined by the UVER values corresponding to solar noon. In a previous paper (10) the authors analysed data from 11 stations in the Iberian Peninsula and found a good agreement with both solar noon and daily maximum. In fact, differences between the two criteria to determine UV Index were less than one unit in 90-96% of cases, depending on the station. Moreover the highest percentage corresponded to stations close to the Mediterranean coast. It was therefore considered reasonable to estimate the UV Index based on the noon values. Table IV shows the UV Index at each measurements station, and its recurrence (in %), over the period under consideration. It can be observed that the maximum UV Index is

10 at the stations of Molló and La Mata because of the altitude and the latitudinal effects, respectively.

Based on the previous data a daily UVER irradiation database (Jm^{-2}) was created. These daily data were used to calculate cumulative doses over the year 2003. The cumulative curves (beginning on 1st January) were obtained by dividing these doses by the SED (Standard Erythemal Dose) (5) and to the MED (Minimum Erythemal Dose) of each phototype. In Fig 3, the results corresponding to the stations of Roses and La Mata are presented. These results represent the irradiances that would be accumulated by an uninterrupted exposure to the Sun throughout the course of the year in a horizontal plane. A change of slope is observed on the plots during summer months. Under these exposure conditions, a Type I skin, for instance, receives approximately 3000 MEDs in a year and about three-quarters of this would come from the summer season. The accumulated doses between the days 90 and 270 (in J/m^2) for a Phototype I skin are of 2350 for Roses and of 2970 for La Mata. In the rest of the year they are of 862 and 910 respectively.

b) Modelled UV Index

Estimates of the UV Index at solar noon have been calculated using the SBDART model for the 9 stations given in Table I every day in the period under consideration. As indicated previously, the model has been applied for cloud-free skies, and has been corrected for altitude but not cloudiness. The estimated values have been compared with each station's experimental UV Index. Fig. 4 shows, as an example, the annual evolution of the daily measured and modelled UV Index for the Valencia station during 2003. The annual evolution of the UVER values, forecast and measured, is shown in

Fig. 5. In this figure the curves show better agreement than in Fig. 4 because here the values for the UV Index evaluation are not truncated.

The plots are almost coincident and there are only substantial disagreements on days in which the experimental UV Index is abnormally low for that season because of cloudy or overcast conditions (high clouds scarcely affect UV irradiance). Considering that the output of the model does not take into account clouds, the result is quite good. For all stations, both index values (measured and modelled) are in agreement or differ by only one unit in more than 81% of cases. This is an acceptable result because the rounding of the index to a whole number alone can mean a one unit difference in UV Index could be the results of a real difference of less than 0.025 W/m^2 in UVER. By using cloudiness data providing by the National Institute of Meteorology and the Catalan Weather Service, days on which low clouds were present could be screened. For the remaining days measured and modelled index values were in agreement to within one unit for more than 90% of the cases for all the stations in the period of measurements. Results are summarised in Table V, finding a total agreement or only one unit of difference between measured and modelled values in the 94% of cases.

The analysis of the deviations show that the SBDART model overestimates the experimental values about a 10%. So the differences between the experimental and estimated values are higher when the incident radiation is higher, according to the fact that in Table V the bottom three sites show a larger 1 UV Index difference than the 0 difference, while the top four sites show the opposite. This circumstance is being considered to introduce the convenient modifications in the prediction model.

CONCLUSIONS

UVER values recorded by the networks of the Catalonia and the Valencian Region, corresponding to 2003 have been analysed. Considering only values that lead to moderate, high or very high UV Index (3 or more), these values show a latitudinal dependence (at sea level) of 3-4% per degree. In the same way, they present an altitude dependence of 10% per km. There are enough analysed values to validate these results. From these measurements, the respective daily UV Indexes have been calculated for each location. Most stations show a maximum UV Index of 9 (very high), except for Molló station (the highest altitude) and La Mata station (with the lowest latitude) where values of 10 were reached.

The measured values are useful to test the accuracy of the UV Index forecast independently by the Catalan Weather Service and the Environment Department of Valencia, using in both cases the SBDART model. In 94% of cases, differences between measured and forecast values, in cloud-free sky conditions, are one or less.

ACKNOWLEDGEMENTS

The UVB radiation measurement network of the Valencian Region is the result of the collaboration between the Valencian Autonomous Government and the University of Valencia through the agreement "Design, installation and fine tuning of a measurement network of the UVB solar radiation in the Valencian Region". M.J. Marín enjoyed a grant subsidized by this agreement. UVB radiation measurement network of Catalonia is the result of the collaboration between the Catalan Weather Service, the University of Barcelona and the National Institute of Meteorology.

REFERENCES

1. Farman J.C., B.G. Gardiner and J.D. Shanklin (1985) Large losses of total ozone in Antarctica reveal seasonal ClOx/Nox interaction. *Nature* **315**, 207-210.

2. ICNIRP, International Commission on Non-Ionizing Radiation Protection (1995) *Global Solar UV Index*, WHO/WMO/UNEP/ICNIRP recommendation, ICNIRP publication 1/95, Oberschleissheim, Germany.

3. WHO, World Health Organization (2002) *Global solar UV Index: a practical guide*. Geneva, Switzerland.

4. McKinlay A.F. and B.L. Diffey (1987) A reference spectrum for ultraviolet induced erythema in human skin. *CIE Journal* **6**, 17-22.

5. ISO 17166 CIE S 007/E (2000) *Erythema reference action spectrum and standard erythema dose*, 4 pp, CIE Publications. Wien, Austria.

6. Mckenzie, R.L., K.J. Paulin and M. Kotkamp (1997) Erythemal UV irradiances at Lauder, New Zealand: relationships between horizontal and normal incidence, *Photochem. Photobiol.* **66**, 683-689.

7. Koepke P. and 23 others (1998) Comparison of models used for UV index calculations, *Photochem. Photobiol.* **67**, 657-662.

8. WMO, World Meteorological Organization (1998) *Report of the WMO-WHO meeting of experts on standardization of UV indices and their dissemination to the public*, W.M.O. Global Atmosphere Watch no 127, WMO/TD No. 921, Switzerland.

9. Madronich, S. (1994) *The need for global UV monitoring*, W.M.O. Global Atmosphere Watch no 95, WMO/TD No. 625, Switzerland.

10. Martínez-Lozano J.A. and 16 others (2002) UV Index experimental values during the years 2000 and 2001 from the Spanish Broad Band UV-B Radiometric Network. *Photochem. Photobiol.* **76**, 281-287.

11. González-Frías C., J.A. Martínez-Lozano, F. Tena, M.P. Utrillas, J. Lorente and X. de Cabo (2002) La red española de medida de radiación UVB. *Rev. Española Fís.* **16**, 18-23. (In Spanish).

12. Martínez-Lozano J.A., F. Tena, M.J. Marín, M.P. Utrillas, J. Lorente, X. de Cabo and C. González-Frías (2002) Experimental values of the UV index during 2000 at two locations in Mediterranean Spain. *Int. J. Climatology* **22**, 501-508.

13. Lantz, K.O., P. Disterhoft, J. J. DeLuisi, A. Thompson, E. Early, D. Bigelow, and J. Slusser (1999) Methodology for Deriving Erythemal Calibration Factors for UV Broadband Radiometers of the U.S. Calibration Facility. *J. Atmos. Oceanic Tech.* **16**, 1736–1752.

14. Leszczynski, K., K. Jokela, L. Ylianttila, R. Visuri and M. Blumthaler (1998) Erythemally weighted radiometers in solar UV monitoring: results from the WMO/STUK intercomparison. *Photocem. Photobiol.* **67**, 212-221.

15. Labajo, A., E. Cuevas, B. de la Morena (ed.) (2004) *The first Iberian UV-Visible instruments intercomparison. Final report*. Ministerio Medio Ambiente Madrid, Spain.

16. WMO, World Meteorological Organization (2001) *Report of the LAP/COST/WMO Intercomparison of erythemal radiometers.* W.M.O. Global Atmosphere Watch no 141, WMO/TD No. 1051, Switzerland.

17. Vanicek, K., T. Frei, Z. Litynska and A. Schnalwieser (2000) *UV-Index for the public, COST-713 Action (UV-B Forecasting)*, Brussels, 27 p.

18. Ricchiazzi P., S. Yang, C. Gautier, D. Sowle (1998) SBDART: A Research and Teaching Software Tool for Plane-Parallel Radiative Transfer in the Earth's Atmosphere. *Bull. Am. Meteorol. Soc.* **79**, 2101-2114.

19. SBDART (2002). Available at: http://www.crseo.ucsb.edu/esrg/pauls_dir. Accessed on 20 June 2003.

20. SBDART (2002). Available at: http://arm.mrcsb.com/sbdart/. Accessed on 20 June 2003.

21. TOMS (2004) http://toms.gsfc.nasa.gov/teacher/ozone_overhead.html. Accessed on 10 January 2004

22. Blumthaler M., W. Ambach and W. Rehwald (1992) Solar UV-A and UV-B radiation fluxes at two alpine stations at different altitudes. *Theor. Appl. Climatol.* **46**, 39-44.

FIGURE CAPTIONS

Figure 1.- Autonomous regions of Catalonia and Valencia in the framework of the Iberian Peninsula and the stations of the measurement networks in both regions.

Figure 2.- 2003 annual evolution of the UVER values at solar noon. (a) Molló; (b) Roses; (c) Barcelona; (d) El Perelló; (e) Prat de Cabanes; (f) Aras de los Olmos; (g) Valencia; (h) Denia; (i) La Mata.

Figure 3.- Irradiation accumulated over the year, expressed in SED (—·—) and in MED for different skin phototypes: (—) Phototype I; (— · · —) Phototype II; (---) Phototype III; (·····) Phototype IV. (a) Roses; (b) La Mata.

Figure 4.- Annual evolution of the experimental (solid line) and modelled (dashed line) UV Index values. Station of Valencia.

Figure 5.- Annual evolution of the experimental (solid line) and modelled (dashed line) UVER values. Station of Valencia.

Figure 1


CATALONIA
REGION OF VALENCIA
Mediterranean Sea


a
b
c
d
e
f
g
h
j
a. Molló
b. Roses
c. Barcelona
d. El Perelló
e. Prat de Cabanes
f. Aras de los Olmos
g. Valencia
h. Denia
i. La Mata

Figure 2

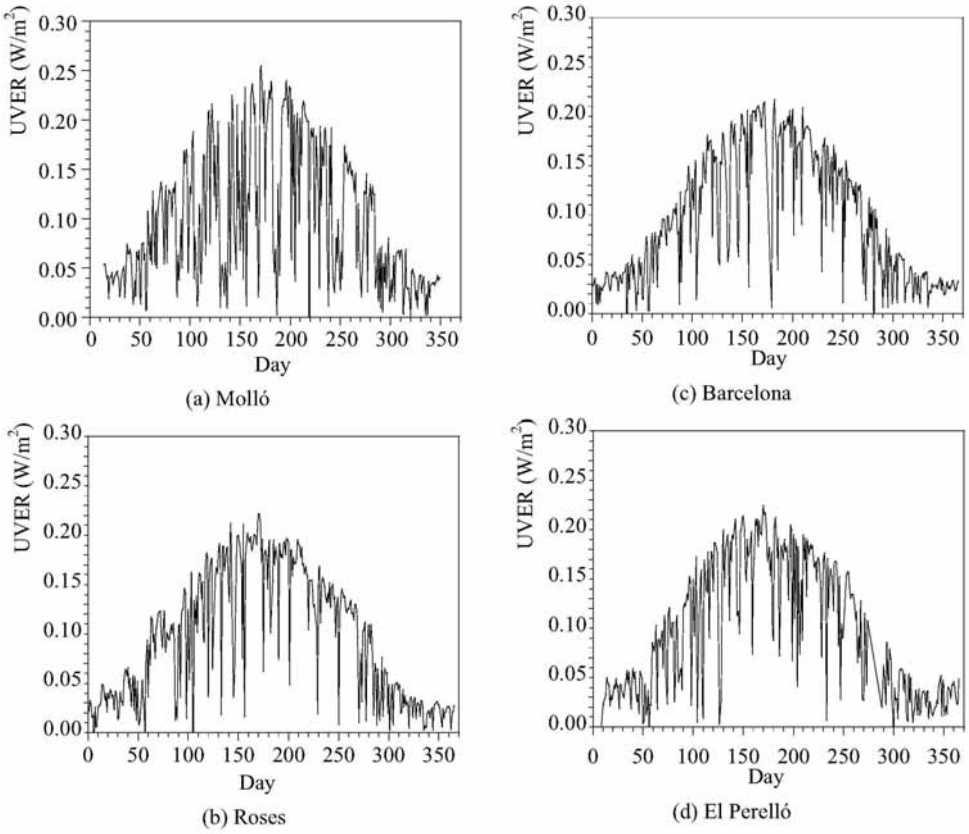
UVER (W/m²)
0.00
0.05
0.10
0.15
0.20
0.25
0.30
0 50 100 150 200 250 300 350
Day
(a) Molló
(c) Barcelona
(b) Roses
(d) El Perelló

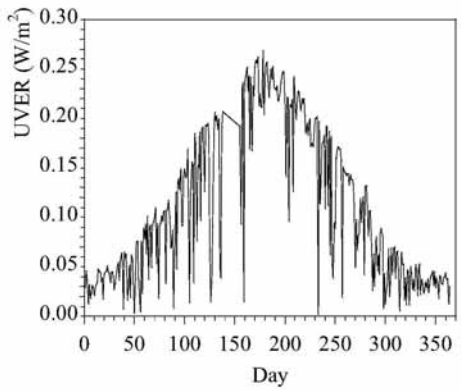

(e) Prat de Cabanes

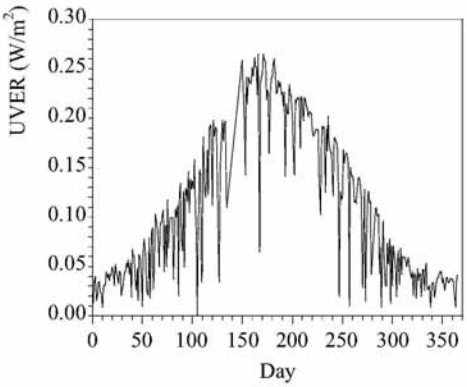

(g) Valencia

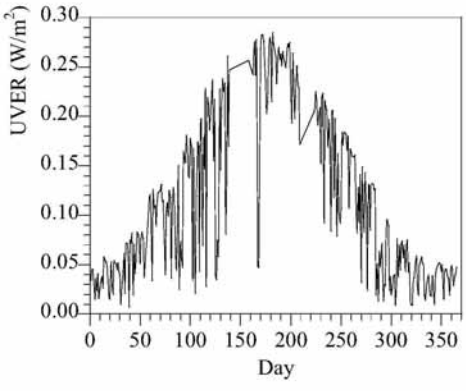

(f) Aras de los Olmos

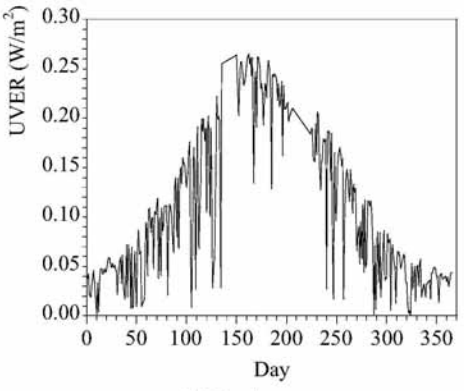

(h) Denia

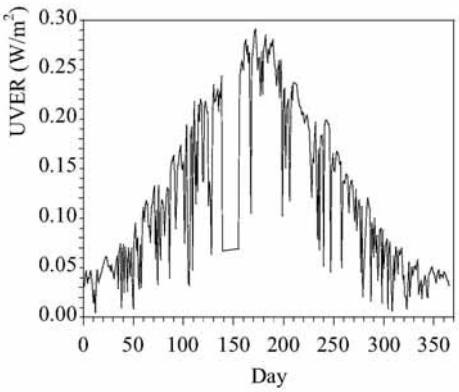

(i) La Mata

Figure 3

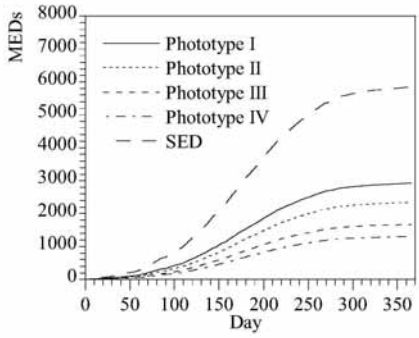

(a) Roses

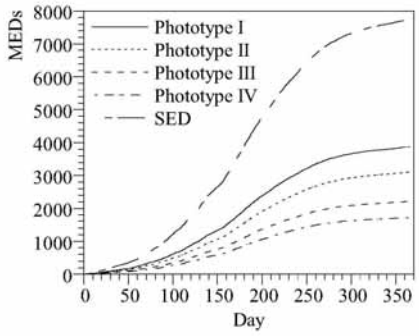

(b) La Mata

Figure 4

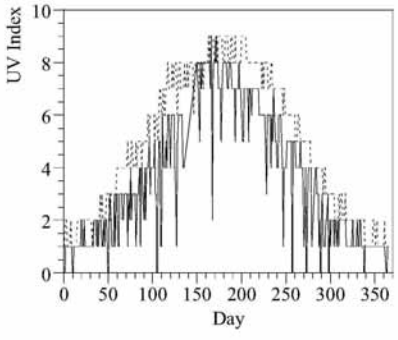

Figure 5

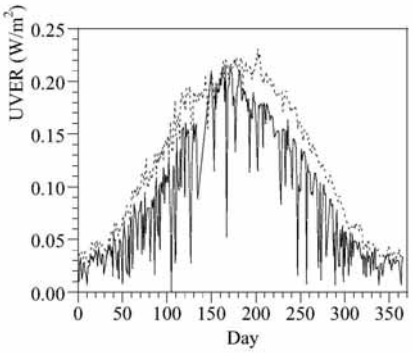

Table I.- Coordinates of the stations of the Catalonian and Valencian networks.

Station	Latitude	Altitude (m a.s.l.)
a) Molló	42º 21' 36" N	1406
b) Roses	42º 16' 16" N	24
c) Barcelona	41º 23' 08" N	98
d) El Perelló	41º 15' 25" N	179
e) Prat de Cabanes	40º 08' 13" N	14
f) Aras de los Olmos	39º 57' 01" N	1277
g) Valencia	39º 27' 49" N	10
h) Denia	38º 49' 19" N	44
i) La Mata	38º 00' 30" N	12

Table II.- Cloud Modification Factor (CMF) for different cloud types and amounts of cloud cover (17).

Cloudiness (octas)	Clear (0-2)	Partial (3-4)	Extensive (5-6)	Overcast (7-8)
High	1.0	1.0	1.0	0.9
Middle	1.0	1.0	0.8	0.5
Low	1.0	0.8	0.5	0.2

Table III.- Monthly mean of cloud-free daily values of UVER (W/m^2) at solar noon for each station.

Erythemal UV (W/m^2)	a) Molló	b) Roses	c) Barcelona	d) El Perelló
January	0.040	0.030	0.032	0.035
February	0.056	0.045	0.045	0.041
March	0.121	0.102	0.090	0.098
April	0.157	0.142	0.140	0.147
May	0.192	0.181	0.175	0.187
June	0.225	0.194	0.199	0.196
July	0.214	0.184	0.187	0.187
August	0.188	0.157	0.167	0.166
September	0.145	0.127	0.132	0.129
October	0.107	0.087	0.073	0.055
November	0.043	0.032	0.041	0.037
December	0.032	0.020	0.028	0.030

Table III.- Monthly mean of cloud-free daily values of UVER (W/m^2) at solar noon for each station. (cont.)

Erythemal UV (W/m^2)	e) P. Cabanes	f) A. Olmos	g) Valencia	h) Denia	i) La Mata
January	0.035	0.037	0.034	0.039	0.041
February	0.051	0.066	0.054	0.057	0.067
March	0.096	0.117	0.103	0.107	0.118
April	0.156	0.178	0.149	0.162	0.172
May	0.195	0.231	0.196	0.218	0.220
June	0.240	0.263	0.242	0.245	0.262
July	0.232	0.259	0.224	0.230	0.248
August	0.197	0.203	0.192	0.183	0.197
September	0.152	0.167	0.144	0.148	0.149
October	0.086	0.098	0.091	0.099	0.095
November	0.051	0.057	0.046	0.050	0.049
December	0.033	0.038	0.033	0.037	0.038

Table IV.- Total days and recurrence percentage (in brackets) that the indicated UV Index value is reached in each station.

Station	UV Index										
	0	1	2	3	4	5	6	7	8	9	10
a) Molló	16 (5)	52 (16)	66 (20)	43 (13)	23 (7)	38 (12)	14 (4)	21 (6)	26 (8)	22 (7)	5 (2)
b) Roses	19 (5)	94 (26)	39 (11)	20 (5)	37 (10)	45 (12)	33 (9)	41 (11)	33 (9)	4 (1)	
c) Barcelona	17 (5)	79 (22)	56 (16)	36 (10)	25 (7)	32 (9)	29 (8)	45 (13)	35 (10)	2 (1)	
d) El Perelló	25 (7)	70 (20)	60 (17)	22 (6)	25 (7)	28 (8)	32 (9)	48 (14)	34 (10)	4 (1)	
e) Prat Cabanes	15 (4)	90 (26)	52 (15)	39 (12)	21 (6)	25 (7)	35 (10)	36 (11)	27 (8)	2 (1)	
f) Aras Olmos	14 (4)	85 (26)	55 (17)	30 (9)	30 (9)	27 (8)	25 (8)	25 (8)	25 (8)	9 (3)	
g) Valencia	10 (3)	99 (29)	47 (13)	29 (8)	42 (12)	28 (8)	31 (9)	34 (10)	24 (7)	2 (1)	
h) Denia	18 (6)	73 (22)	60 (18)	29 (9)	34 (10)	30 (9)	25 (8)	22 (7)	33 (10)	2 (1)	
i) La Mata	6 (2)	65 (19)	65 (19)	27 (8)	39 (11)	30 (9)	19 (6)	36 (10)	19 (6)	30 (9)	5 (1)

Table V.- Number of cases (in %) in which the difference between experimental and modelled index is related on the top of the Table.

Station	Difference		
	0	1	2
a) Molló	47.5	45.0	7.4
b) Roses	61.9	36.8	1.4
c) Barcelona	57.1	41.0	1.7
d) El Perelló	54.9	43.9	1.2
e) Prat de Cabanes	42.8	53.4	3.8
f) Aras de los Olmos	52.5	47.1	0.4
g) Valencia	31.8	58.5	9.7
h) Denia	40.6	54.3	5.1
i) La Mata	40.9	55.5	3.6

C.2 International Radiation Symposium. Proceedings, 2004

ALTITUDE EFFECT ON UV INDEX DEDUCED FROM THE VELETA-2002 EXPERIMENTAL CAMPAIGN (SPAIN)

J. LORENTE, X. DE CABO, E. CAMPMANY, Y. SOLA.
Dept. de Astronomía y Meteorología, Universitat de Barcelona, Spain (jeroni@am.ub.es)

J.A. GONZÁLEZ, J. CALBÓ, J. BADOSA. Dept. de Física. Universitat de Girona, Spain
L. ALADOS-ARBOLEDAS. Grupo de Física la Atmósfera, Universidad de Granada, Spain
A. MARTÍNEZ-LOZANO. Grupo de Radiación Solar, Universitat de Valencia, Spain
V. CACHORRO. Grupo de Óptica Atmosférica, Universidad de Valladolid, Spain
A. LABAJO. Instituto Nacional de Meteorología, Spain
B. DE LA MORENA. Estación de Sondeos Atmosféricos de El Arenosillo, INTA, Huelva, Spain
A.M. DÍAZ. Dept. de Física Básica, Universidad de La Laguna , Spain
M. PUJADAS. Dept. de Impacto Ambiental de la Energía. CIEMAT, Spain
H. HORVATH. Experimental Physics Institute, University of Wien, Austria
A.M. SILVA. Dept. de Física. Universidade de Évora, Portugal
G. PAVESE. CNR-IMAA, Italy.

ABSTRACT

During the 2002 summer the Veleta-2002 experimental campaign was undertaken at the Sierra Nevada Massif, close to Granada in the South-Eastern of Spain. Measurements of UV solar spectral irradiance, UVB broad-band irradiance, ozone, aerosol optical depth (AOD) and other optical properties of the atmosphere were carried out at both slopes of the Sierra Nevada Massif, covering an altitude range of 0-3398 m above sea level (a.s.l.). During the campaign the UV altitude effect was determined. Results for cloudless conditions and small zenith angles show an altitude effect around 9 % km^{-1} in the UVB solar irradiance while this effect on UV Index (UVI), based on biologically effective irradiance, ranges 11-14 %km^{-1} depending on the SZA. There is a strong relation between atmospheric turbidity and altitude effect, so those intervals are higher when AOD increases. However UVI values show an important diurnal evolution, mainly in hours with high values of AOD. At noon, the maximum UVI observed at different altitudes ranges from around 8 at the lower measurement point to 12 at Veleta Peak (3398 m a.s.l.).

1. INTRODUCTION

The knowledge of solar UV radiation reaching the Earth's surface has a great interest because of its significant role in atmospheric and biological processes. This radiation is influenced by diverse factors like the atmospheric ozone content, aerosol particles, cloudiness, surface albedo and altitude. This last factor is the goal of our study. Solar radiation increases with the altitude because of the decrease of its attenuation due to absorption and scattering by air molecules, aerosols and clouds. The *UV altitude effect* (UVAE) is defined as the increase of UV solar irradiance with altitude due to the shorter path length of solar beam through the atmosphere and it is generally expressed as the relative irradiance increase (in % per km) between the higher to the lower site (Blumthaler et al., 1997). Several UVAE investigations have been carried out in different places during recent years showing a wide range of values (2-25% km^{-1}) depending on UV wavelength, solar zenith angle, air mass type, surface cover and season (Blumthaler et al., 1997; McKenzie et al., 2001; Pfeifer et al., 2003). Atmospheric turbidity is one of the main important factors contributing to UVAE variation. When the air in the surface of lower sites is much polluted the UVAE increases considerably. McKenzie et al. (1997) report significant smaller UVAE values from comparisons between two clear sites, Lauder (New Zealand) and Mauna Loa Observatory (Hawaii), showing the effect of low altitude pollution on UV differences.

At the beginning of summer 2002, the VELETA-2002 experimental campaign (Alados-Arboledas et al., 2002) was undertaken at the Sierra Nevada Massif, close to Granada city in the South-Eastern of Spain (Figure 1). One of the main goals of the campaign was the evaluation of aerosol impact on UV solar radiation.

Measurements of UV solar spectral global irradiance, UVB broad-band irradiance, ozone, aerosol optical depth (AOD) and other optical properties of the atmosphere were carried out at both slopes of Sierra Nevada Massif, covering an altitude range between 10 and 3398 m a.s.l.

In order to assess the quality of the measurements from the whole campaign, a common calibration with laboratory lamps and exhaustive intercomparisons between different kind of spectroradiometers (Brewer MK-IV, Bentham DM150, Oriel and Optronic 754) and broadband UVB radiometers (Yankee UVB-1) were performed during the first stage of this field campaign.

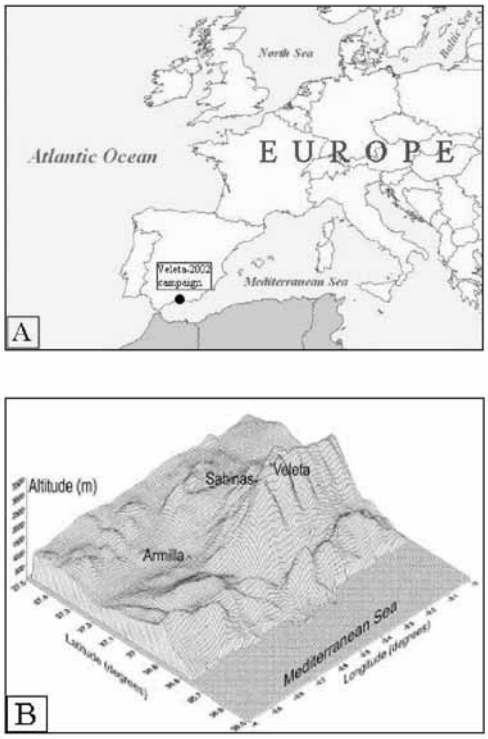

Fig. 1: Details of the Veleta 2002 campaign. A) Geographical location. B) Topography of the zone showing different points of measurements.

Figure 2 shows one of these intercomparisons and spectral irradiances measured at different altitudes during the second stage. Due to the specific optical characteristics of each instrument, the spectra of solar irradiance have been standardised to a 1nm FWHM triangular slit using the SHICrivm program (Slaper, 1997). This software tests and calibrates the outputs of different kinds of sensors.

In addition daily sounding profiles of temperature, humidity, wind and ozone as well as LIDAR measurements were achieved.

Here we present some of the results of UVAE calculations for UV spectral, UVB integrated and biologically effective irradiances at the Northern slope of the Sierra Nevada Massif. This last was both obtained from spectral measurements weighting by the erythema action spectrum (McKinlay and Diffey, 1987), also known as CIE action spectrum. Frequently this biologically effective irradiance is expressed as UV index (UVI), multiplying its values in W m^{-2} by 40/(W m^{-2}) (Vanicek et al., 2000).

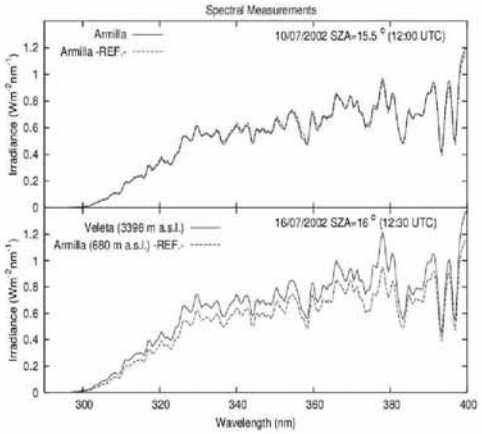

Fig. 2: Spectral measurements during the campaign. On the top, it is shown the spectral distribution of UV solar irradiance corresponding to two different spectroradiometers measuring at the same site (Armilla) during the intercomparison stage. On the bottom, the spectral distributions corresponding to simultaneous measurements in two different altitudes: Armilla and Veleta Peak

2. RESULTS OF UV ALTITUDE EFFECT CALCULATIONS

Simultaneous measurements of UV spectral irradiance at different altitudes for cloudless conditions showed a considerable variation of UVAE.

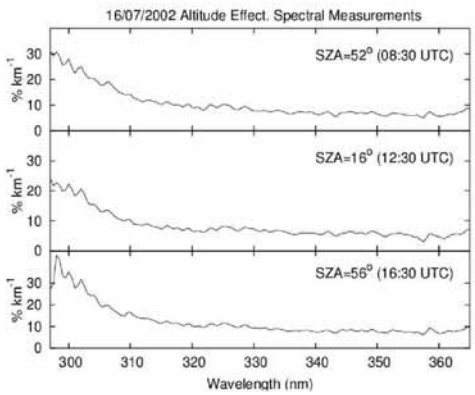

Fig. 3: Spectral altitude effect obtained from relative differences (% km^{-1}) between spectral measurements at Veleta Peak and Armilla for three different SZA during the same day.

UVAE shows a different behaviour depending on the spectral band. In the UVB wavelength interval there is a high dependence of UVAE with wavelength since it ranges from 30 %km^{-1} to 5 %km^{-1}. Differences are highest when SZA increases. In the UVA wavelength range (320-400 nm), the altitude effect variations with SZA or wavelength are less and values are between 5 and 10 %km^{-1}.

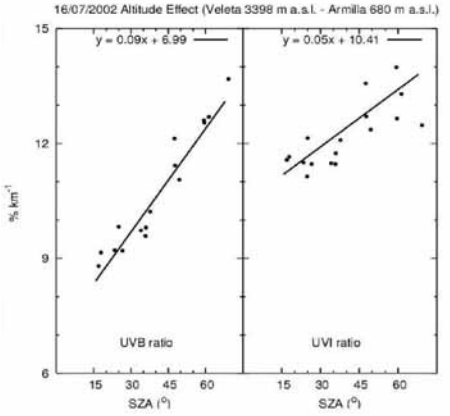

Fig. 4: Altitude effect versus SZA obtained from relative difference (%km^{-1}) between integrated magnitudes (UVB and UVI) of spectral irradiances measured by spectroradiometers

UVAE shows values from 8 %km^{-1} to 13 %km^{-1} for integrated UVB. In the case of UVI based on biologically effective irradiance, the slope of the lineal tendency is less due to the influence of wavelengths in the UVA wavelength interval. The UVAE ranges 11-14 % km^{-1} but the measurements do not show such a good correlation.

These last values are higher to the 8 %km^{-1} recommended by COST Action 713 (Vanicek et al., 2000). One of the reasons of this fact is that the UVAE has a strong dependence with atmospheric turbidity. Little variations of the amount or the optical properties of the aerosols in one of the points of reference can introduce differences in UVAE since there are changes in the solar spectral irradiance measured.

3. ALTITUDE EFFECT AND AEROSOL OPTICAL DEPTH

In the literature there are several works about the UVAE based on the study of data measured at different place of the world. The result is a wide range of values depending on the specific atmospheric turbidity during the period of measurement.

The Veleta-2002 campaign lasted some days, so different atmospheric situations were observed. From the spectral irradiance and photometric measurements, AOD has been determined to characterize the turbidity.

The highest variations were recorded at the lowest point due to the pollution of the city. On the other hand at highest altitudes, differences are less significant (Figure 5).

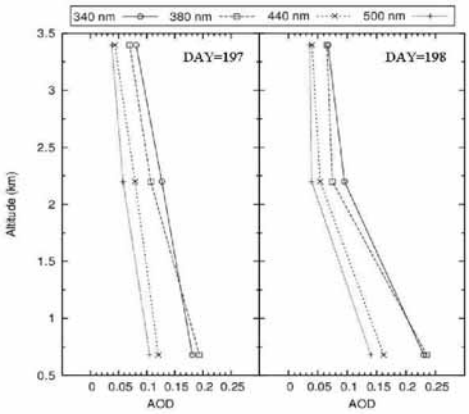

Fig. 5: AOD profiles from simultaneous measurements at the points of observation during two days of the campaign at 12:30 UTC (SZA=16°)

These variations in AOD are reflected in the spectral altitude effect (Figure 6). When the turbidity increases at the lowest point, the UVAE is higher. Although there are differences in the entire UV spectrum, these are high in UVB range and less appreciable in UVA one.

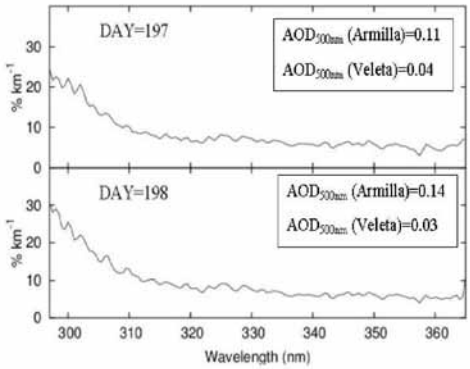

Fig. 6: Spectral altitude effect for two days of the campaign

For measurements with the same SZA, 16º, UVAE in UVI is 11.6 %km^{-1} in day 197 and 14.0 %km^{-1} in day 198 when the turbidity was high.

After studying the UVAE calculated from different altitudes, that it can not be described by a single number because of the close relation with aerosols (type and amount).

4. CONCLUSIONS

UV altitude effect observed during the VELETA 2002 campaign shows a significant and complex variability with wavelength and SZA, increasing strongly for high turbidity conditions in the lower places. The main features of altitude effect are that it increases at shorter wavelengths and with high SZA, respectively. SZA dependence produces an important diurnal evolution of UVAE, mainly in hours with high values of AOD.

Therefore, in agreement with other studies, this effect can not be described by a single percentage of increase applied to the altitude variation. Therefore, in order to apply a realistic correction of UV index for different altitude sites, an appropriate characterisation of the air mass turbidity will be necessary.

AKNOWLEDGMENTS

This work was supported by "La Dirección General de Ciencia y Tecnología" from the Education and Research Spanish Ministry through coordinated project No: CLI200-0903-C08.

REFERENCES

Alados-Arboledas, L. F.J. Olmo, J. Lorente, J.A. Martínez, V. Cachorro, C. González Frías, B. De la Morena, J.P. Díaz, M. Pujadas, 2002: VELETA 2002 Field Campaign. *Proc. 3ªAsamblea Hispano Portuguesa de Geodesia y Geofísica*, Valencia 1189-1193.

Blumthaler, M., W. Ambach, R. Ellinger, 1997: Increase in solar UV radiation with altitude. *J. Photochem. Photobiol. B*, 39, 130-134.

McKenzie, R., L., P.V. Johnston, D. Smale, B.A. Bodhaine, S. Madronich, 2001: Altitude effects on UV spectral irradiance deduced from measurements at Lauder, New Zealand, and at Mauna Loa Observatory, Hawai. *J. Geophys. Res.,* 106(D19), 22845-22860.

McKinlay, A.F., B.L. Diffey, 1987: A reference action spectrum for ultraviolet induced erythema in human skin. *CIE J.*, 6, 17-22.

Pfeifer, M., P. Koepke, J. Reuder, F. Wagner, 2003: Dependence of UV radiation on altitude and aerosol optical depth: example Bolivia. *Geophysical Research Abstracts,* Vol. 5 08862, EGS.

Slaper, H., 1997: Methods for intercomparing instruments. *Advances in solar ultraviolet spectroradiometry,* European Commission. Air pollution research report 63, Luxembourg, 155-164

Vanicek, K., T. Frei, Z. Litynska, A. Schmalwieser, 2000: UV-Index for the Public. *COST-713 Action*. European Communities 27 pp.

C.3. The first Iberian UV-Visible instruments intercomparison. Final report, 2004; Chapter 10, 101-108

C.3 The first Iberian UV-Visible instruments intercomparison. Final report, 2004; Chapter 10, 101-108

CHAPTER 10
MODELING

Xabier de Cabo, Elies Campmany, Miguel Martín and Jerónimo Lorente
Department of Astronomy and Meteorology, University of Barcelona

SUMMARY

Four radiative transfer models of different complexity (two advanced multiple scattering radiative transfer models and two simple radiative transfer models) have been used to compare their simulations with the measurements carried out during *El Arenosillo '99* intercomparison campaign. The average of the global irradiance measurements (spectral irradiance, UV-A and UV-B integrated radiation) carried out with two well-calibrated double monochromator spectroradiometers Bentham 150, (see chapter 5 for details) at the same location and at the same time over a range of different zenith angles, has been taken as a reference for the comparison with the outputs of the models. In addition to meteorological variables like atmospheric pressure, temperature and relative humidity, aerosol optical properties (single scattering albedo, asymmetry parameter, Angström turbidity parameters and aerosol optical depth) at different wavelengths, total ozone and solar zenith angle were known and were provided as input parameters.

The models have a good agreement with measurements for zenith angles lower than 60°. In this last case the differences between models and instrumental measurements of UV index (UVI) are about ±15% depending on the model (corresponding roughly ±0.8 UVI units). These differences are quite good if we consider the usual measuring uncertainty (±10%) and the fact that UVI is meant for distribution to the public.

10.1. INTRODUCTION

The use of radiative transfer models to study the UV solar radiation reaching the earth's surface has a great interest for different reasons. One would be the need of the knowledge of the solar UV doses which population is exposed in different environments as a consequence of the observed decrease of ozone column. However, there are still few places that have the appropriate measurements of this radiation, i. e., there is a lack of a suitable UV network which let us know the distribution of UV solar irradiance, including its variable spectral composition and hence its variable erythema. The main causes of the scarce UV network are the high prices of instrumentation and the need of periodic calibrations and personal dedication for monitoring the measurements of these delicate instruments. Therefore, in order to obtain representative UV data for every place and carry out a daily forecast of such UV doses appears necessary the use of radiative transfer models which would simulate of this radiation for specific places and atmospheric conditions. On the other hand, the use of simulation models is an important tool in atmospheric research and helps us in the understanding of the different processes involved in the solar radiative transfer.

Modeling at UV wavelengths is more complex than longer wavelengths because at shorter wavelengths the influence of ozone column variations becomes very important and because an important proportion of scattered radiation results from shorter wavelengths. This makes Rayleigh scattering more effective as wavelength decreases. One cause of the uncertainty in the output of a certain radiative transfer model is due to model formulation and parameterizations but another factor lies with the uncertainty in the input parameters. *Schwander et al.* (1997) have studied the uncertainties in modelled UV irradiances due to this fact, showing values between 10 and 50% for spectral irradiances depending on wavelength. *Weihs and Webb* (1997) show that this uncertainty could be considerably higher than the uncertainty in measurements for typically available input data. Therefore, to validate models it is necessary to have good measurements of the atmospheric parameters used as input data and, at the same time, also to have good spectral measurements. In the Arenosillo intercomparison campaign we had both.

Different works have been devoted to UV modeling and comparisons with observations. *Mayer and Seckmeyer* (1997) carried out a systematic long-term comparison between UV measurements and model results. The UV measurements were achieved with a Bentham double monochromator spectroradiometer, and the radiative transfer model was the UVSPEC, a freely available software package based on discrete algorithm DISORT. Their comparisons show systematic differences between measured and modeled spectral irradiances in the range −11 and 2% for 295-400 nm wavelength interval and solar zenith angles up to 80°.

In the frame of COST Action 713 (UVB Forecasting) an interesting model comparison exercise was carried out (*Koepke et al.*, 1998). Eighteen radiative transfer models in use for the UV index (UVI) calculation were compared with respect to their results for more than 100 experimental clod-free atmospheres and different zenith angle combinations, although they made no comparison with instrumental measurements.

Models were classified into three groups: 1) multiple-scattering spectral models, which generally take into account multiple scattering and vertical atmospheric inhomogeneity, considering the atmosphere like a superposition of layers where absorption and scattering of radiation take place; 2) fast spectral models, based generally on the atmospheric transmittance method, where the atmosphere is considered as only one layer and simulations require very short time; 3) empirical models, which include direct parameterizations in the input data for the UV calculations. The main conclusion of this comparison exercise were the good agreement in the UV index simulations between the multiple-scattering models: they agree in ±0.5 UV index values in more than 80% of the atmospheres considered in the study. This is indeed a good result because modeling includes, besides the formulation of the models, a number of constants like extraterrestrial solar irradiance and the absorption properties of atmospheric gases and aerosols. The fast models show a very different agreement and the empirical models show good results but only for the atmospheric conditions for which they were developed.

Comparisons between model outputs with measurements are important tasks in order to validate the models. In the frame of mentioned COST Action 713, *De Backer et al.* (2001)

show an exhaustive comparison using the UVI measures from five different instruments at four locations with different latitude and climate and UVI simulations from 13 models but only location, total ozone and solar zenith angle were provided as input parameters. Due to this situation the modelers had to decide what meteorological parameters, aerosol and albedo they should use. Moreover, most instruments do not measure up to 400 nm and it was necessary to do some interpolation. In these comparisons we have observed a big discrepancy between the outputs when we only slightly changed the aerosol optical properties or the ozone values, always using the same model. This has been confirmed by other authors (*Mayer et al.*, 1997; *Pachart et al.*, 1997; *Weihs and Webb*, 1997; *Lorente et al.*, 1994).

In this chapter, four radiative transfer models of different complexity have been used to compare their simulations with the measurements carried out during the campaign.

10.2. METHOD

During the campaign the following atmospheric variables were available:

- Total ozone column obtained by means of measurements from Brewer spectrophotometers.
- Meteorological variables, like atmospheric pressure, temperature and relative humidity.
- Diverse of optical properties of aerosols like single scattering albedo, asymmetry factor, Angström turbidity parameters and aerosol optical depth (AOD) at different wavelengths. Most of these aerosol parameters were calculated from direct irradiance measurements carried out with two spectroradiometers Li-Cor 1100 and two different photometers, Microtops II and Cimel (see chapters 7 and 9).

The knowledge of these input parameters has been very important to obtain better fitting between the models and the measurements which only worked with standard input values. The spectral irradiance measurements used for comparisons were the average of those corresponding to two spectroradiometers Bentham 150 which were operating simultaneously. These instruments, as it is explained in the fifth chapter, presented a good calibration and we also had their slit function.

Taking into account that we only had measurements of two days which did not correspond at the same cloudy situation, we do not show any statistic study. The first day (3.rd of September, day 246) was a cloudless day, whereas the second day (4.th of September, day 247) the cloudiness until noon was between 1/8 and 2/8 of small *cumulus*. During these last measurements the clouds did not cover the sun but they incremented slightly the global irradiance because the appreciable increment of diffuse irradiance which these clouds produced. The few measurements with clouds covering the sun were easily detected by means of the notes taken during the measurements and with the spectral graphics of global irradiance. An example of a measurement with clouds covering the sun, although only for few seconds, can be seen in Figure 9.1 which corresponds at 11:30 UTC of day 247 but it has not been used for the comparison.

From all of the measurements made on 3.rd and 4.th of September we have selected those corresponding, approximately, at 80°, 60°, 45° and 30° zenith angles because these are usually used in model comparisons. Ten daily measurements (five before noon and five after noon) of spectral irradiance in the wavelength interval from 290 nm to 400 nm with spectral resolution of 0.5 nm were considered. The spectral resolution used in the models was 1 nm because it is the maximum resolution of some of the models used.

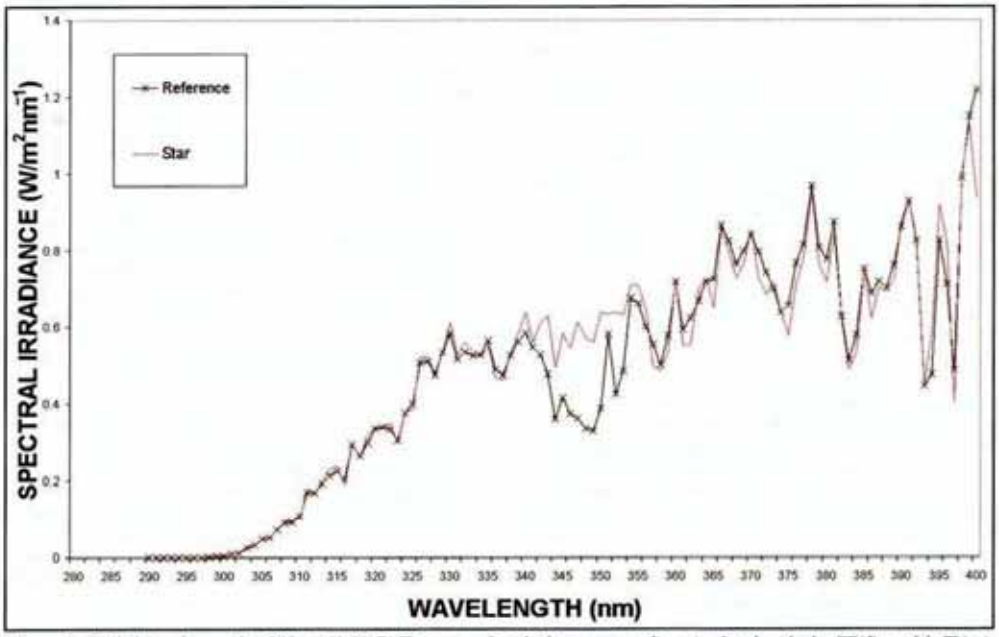

Figure 1. *Global irradiance day 247 at 11:30 GMT compared with the corresponding simulated with the STAR model. This is an example of a measurement with clouds covering the sun during few seconds. While the spectroradiometer is scanning between 340 and 350 nm, the irradiance is lower than it should be.*

The model inputs were: zenith angle; temperature, atmospheric pressure and relative humidity at station level, total ozone column, β and α Ångström parameters, aerosol optical depth (AOD) at 350 nm, 500 nm and 550 nm. Also, when a selected reference atmosphere was necessary, we chose the standard mid latitude atmosphere. For the aerosol atmosphere we considered an oceanic or maritime type. The albedo was of 0.1 for the whole UV spectrum because it is the one that corresponds to forest (pine tree) surface like that which surrounded the whole measurement zone.

To make the comparison we have calculated the absolute and relative differences between models and reference values for ultraviolet index (UVI) and UVA and UVB integrated irradiances. The spectral irradiance from 290 to 400 nm has been considered as well.

The UV index is dimensionless and is defined as:

$$UVI = 40 \int_{250}^{400} I_\lambda \cdot \varepsilon_\lambda \, d\lambda \qquad [9.1]$$

where I_λ is the spectral irradiance at wavelength λ and ε_λ is the CIE action spectrum (*McKinlay and Diffey*, 1987).

10.3. THE MODELS

Four radiative transfer models were used in this work:

a) Two multiple scattering spectral models:

SBDART (***Santa Barbara Disort***) based on a discrete ordinates radiative transfer module (*Stammes et al.*, 1988) and a low atmospheric transmission model with solar data from LOWTRAN7 (*Kneizys et al.*, 1988).

STAR (***System for Transfer of Atmospheric Radiation***) (*Ruggaber et al.*, 1994), developed by the Meteorological Institute of the University of Munich. It is based on matrix operator theory.

b) Two simple spectral models:

SMARTS2: Simple model for the atmospheric radiative transfer of sunshine (*Gueymard*, 1995), is a spectral solar irradiance model based on simple transmittance parameterization of relevant atmospheric parameters.

UVA-GOA, developed by the *Grupo de Óptica Atmosférica* (GOA) (University of Valladolid). The program accounts for the absorption and scattering processes in a single atmospheric layer, but no interaction between both processes has been considered. Single scattering albedo and asymmetry parameter are input parameters and not dependent on wavelength. The aerosol optical depth is given by the Ångström β and α turbidity parameters.

10.4. RESULTS OF THE COMPARISON BETWEEN MODELS AND MEASUREMENTS

10.4.1 UV Index comparison

Multiple scattering models generally show greater UVI values than measured values. This effect has been described in other comparison works (*De Backer et al.*, 2001). We have also observed that the opposite effect happens if we work with simple spectral models and they show lower values than measured ones. Figure 9.2 shows absolute differences between the UVI measured values and the UVI calculated by means of the four models. Around noon, when the UVI reaches its daily maximum values, SMARTS2 and UVA_GOA models always show UVI lower than measurements (between –0.4 and –0.8 UVI units). However, multiple scattering models always produce higher values and with a similar magnitude (between +0.8 y +0.4 units).

It must be noted the opposite behaviour that show these absolute differences in the two days: they are large for multiple

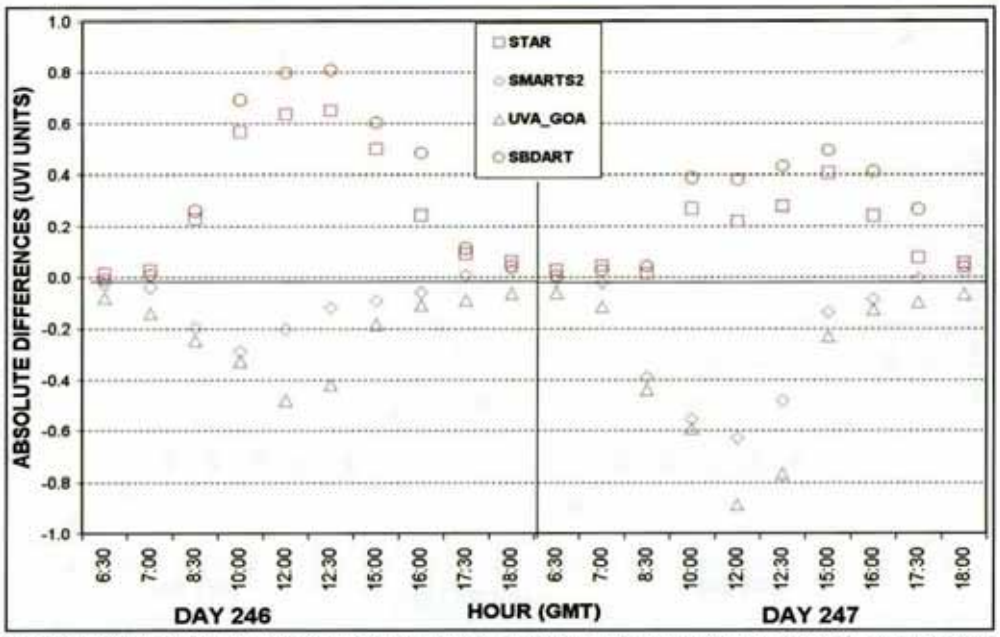

Figure 2. Diurnal evolution of UVI absolute differences between simulations and experimental values during the campaign. These absolute differences are greater around noon, because the UVI has a higher value. The two multiple scattering models overestimate the reference, while simple models are under it.

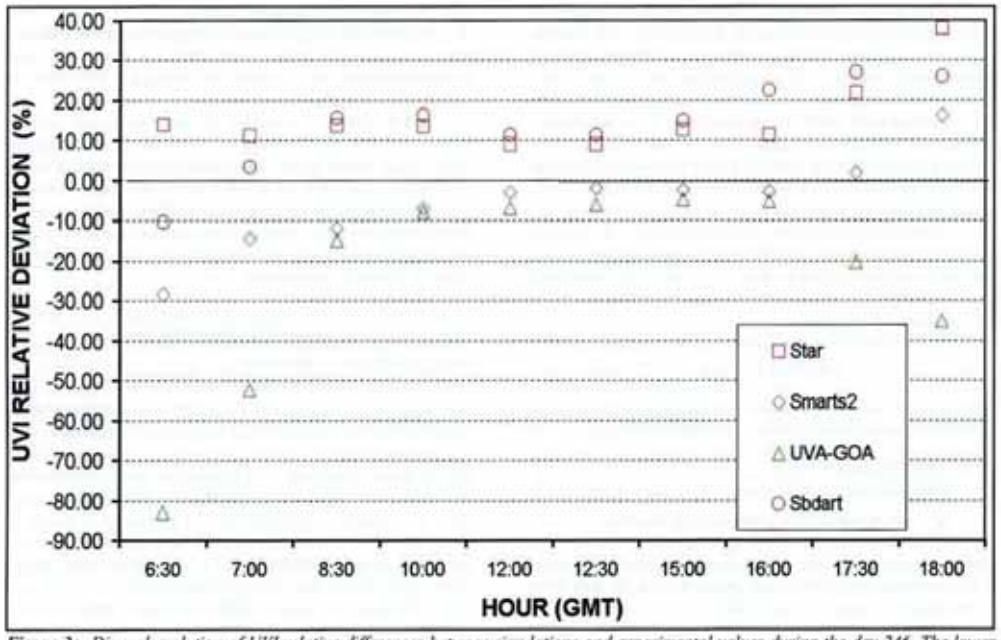

Figure 3a. *Diurnal evolution of UVI relative differences between simulations and experimental values during the day 246. The lower values are observed during noon, just the opposite behaviour than the absolute values. Simple models, specially UVA_GOA, have larger differences with the measurements for great zenith angles.*

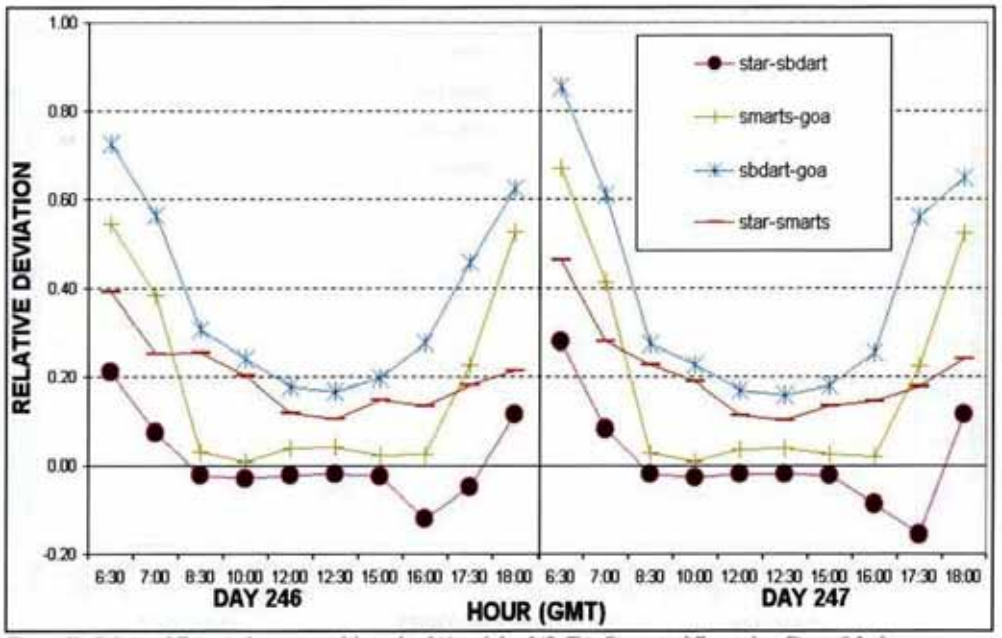

Figure 3b. *Relative differences between models in day 246 and day 247. This Figure is different than Figure 9.3a because we are just comparing the model outputs, but not models with experimental values. As one observes, the lower values correspond to comparison between the two multiple scattering models (SBART and STAR), specially around noon. The higher differences are found between SBDART and UVA_GOA.*

scattering models the first day but the opposite happens for the second day. This is due to the different treatment of scattering for the models when they calculate the diffuse irradiance together with the clouds that were present all the morning which produced an appreciable increment of diffuse irradiance but not a sensible decrease of direct irradiance and, as a result, an increment of global irradiance. For this reason, the UVI values calculated from instrumental measurements are higher for the second day and show a better agreement with the multiple scattering models. Nevertheless, for the cloudless day, they are the simple spectral models which fit better to instrumental measurements (SMARTS2 approximately −0.2 UVI units). Bearing in mind that the UVI is presented to public in entire values, only a maximum difference of ±1 UVI unit could exist between the four models.

Figures 9.3a and 9.3b show the UVI relative differences between modelled and measured values. For the hours near the noon, these differences range between +5% and +15% for multiple scattering models and between −2% and −12% for simple spectral models. Furthermore, we can observe that for zenith angles greater than 60° these differences are very large but as they correspond to little values of UVI they have no influence in the possible biologic effect on people. It must also be kept in mind that the own error of the instrument is about 10%.

In Figure 9.4 we compare the modelled UVI with the observed values and, also, the mean value of all the models.

10.4.2 UVA and UVB global irradiance comparisons

We also have studied the absolute and relative differences between models and observations for the integrated values of global irradiance in UVB and UVA spectral intervals. For the UVA irradiance we can observe that relative deviation is lower than ±10% for zenith angles lower than a 60° (Figure 9.5). For the UVB irradiance and for the same zenith angles, relative deviation has slightly higher values but always lower than ±16%.

Figure 9.6 shows the UVA integrated irradiance. We can see the slightly higher observed values for the second day: about 12% in the two hours before noon, which agrees with the presence of some Cu, and only between 2% and 4% after noon when Cu had disappeared. This effect hardly is present in UVB integrated irradiance (Figure 9.7) where the differences between UVB values of two days is hardly ever between ±2%.

When we only compare model irradiances for two days, UVA and UVB irradiance values are nearly the same because simple spectral models do not consider clouds and furthermore, we did not consider them in multiple scattering models. Only at noon, we can observe for day 247 about 1% lower irradiance values than the first day.

10.4.3 Comparison between models

The UVI differences between multiple scattering models are around 2 or 3% for zenith angles lower than 60°, although they can reach values higher than 12% for low sun elevations. These differences are in agreement with the presented in the Koepke et al. (1998) intercomparison work. For simple spectral models these differences are about 2 and 4% and higher than 20% at the same previous conditions. But when we compare both type of models themselves the differences catch up values between 14-20% for solar zenith angles lower than 60° and greater than 35% for zenith angles higher 60°. It must also be kept in mind that multiple scattering models always give higher irradiance values than simple spectral models.

For UVB integrated irradiances the differences between models are much similar at UVI ones, and for UVA these

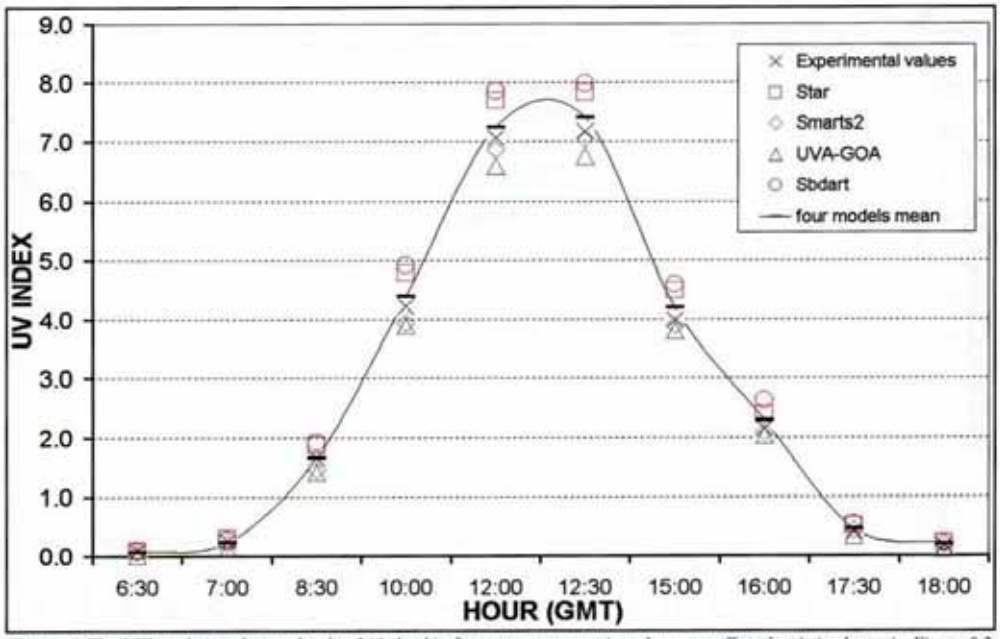

Figure 4. *The UVI evolution during the day 246. In this figure we can apreciate the same effect that it is shown in Figure 9.2, i.e., the multiple scattering models overestimate the UVI and the simple models underestimate it.*

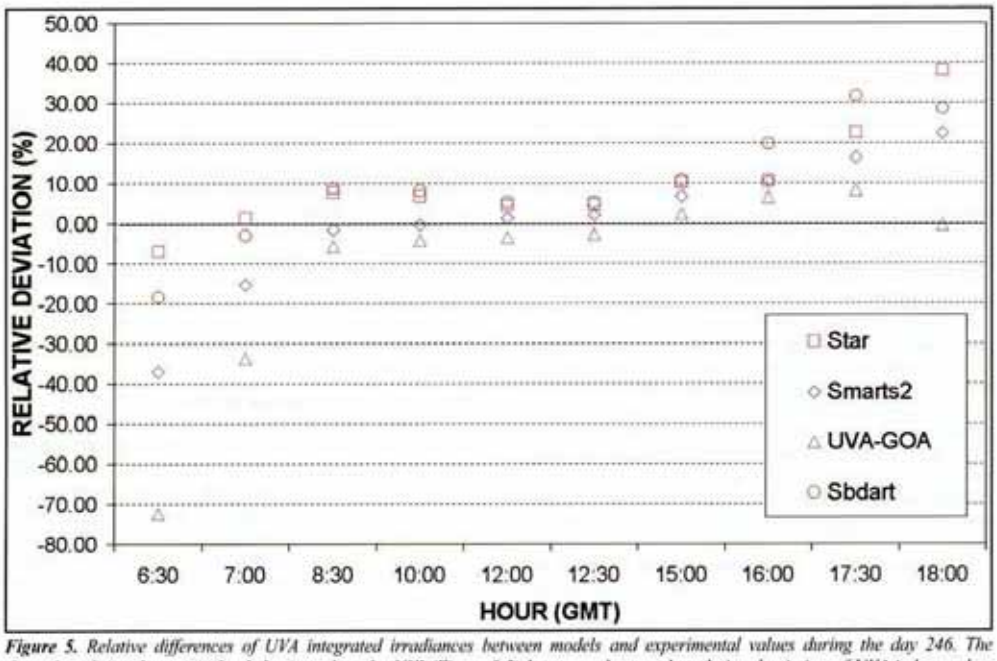

Figure 5. *Relative differences of UVA integrated irradiances between models and experimental values during the day 246. The diurnal evolution has a similar behaviour than the UVI (Figure 9.3) but around noon, the relative desviation of UVA is lower than the UVI relative desviation.*

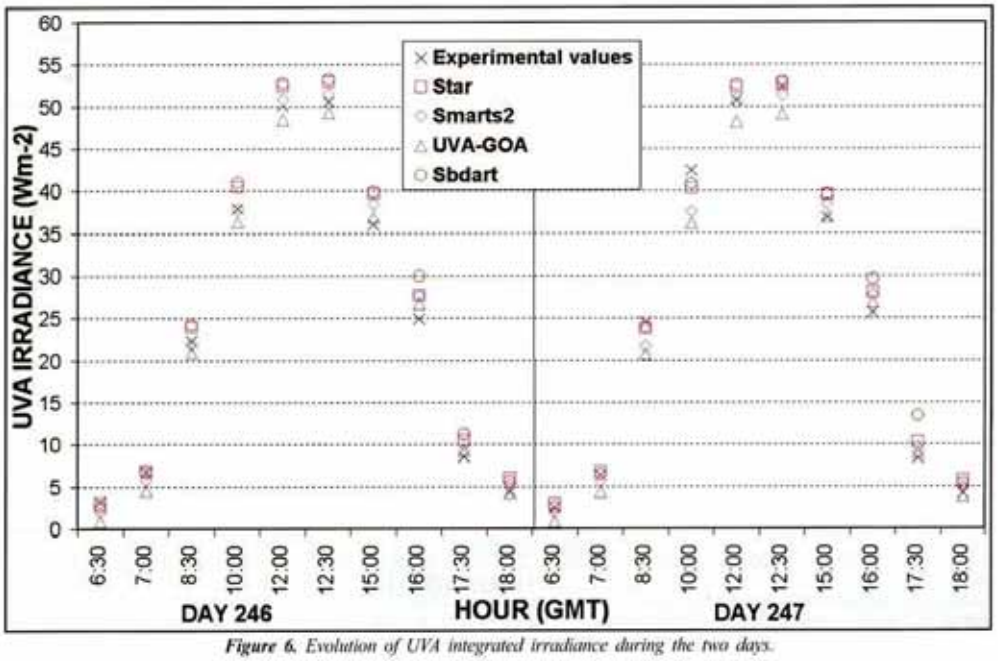

Figure 6. *Evolution of UVA integrated irradiance during the two days.*

differences are lower: only 1% between multiple scattering models and about 3-13% between multiple scattering models and simple spectral models. In Table 1 we can see and average of these deviations. A model sorting (classification) in increasing order of UVA and UVB irradiance values would be the following: UVA-GOA, SMARTS2, STAR and SBDART.

Table 1. *Relative Average Deviation between multiple scattering models (MSM), simple spectral models (STM) and between both (MSM and STM).*

	Relative Average Deviation for 0<60°		
	Between MSM	Between STM	Between Both
UV Index	2%	3%	14%
UVB irradiance	5%	3%	18%
UVA irradiance	1%	4%	6%

If we study the spectral output of the models we can observe they are close together for solar zenith angles 60°. We do not present these figures because there are not distinguishable differences. Only for low sun elevations it is possible to observe that simple spectral models, specially UVA_GOA model, show lower values than reference and multiple scattering model.

10.5. CONCLUSIONS

In this chapter we have applied different models to simulated spectral irradiance during two days in the Arenosillo campaign. Simulations have been compared with observed values of UV spectral irradiances and with the UVI. Although the short period of measurements and the different clear sky conditions observed during the two days, can restrict the validity of the conclusions, some of them appear clearly, like the high uncertainty of all the models for low solar zenith angles. But, for these two days and for zenith angles lower than 60°, the results show a good agreement between models and measurements and between models too. Simple spectral models always underestimated spectral irradiance whereas multiple scattering models overestimated it. As a consequence of this a UV index underestimating will result if we work with simple spectral models. A more exhaustive comparison of modelled results with measurements in different places and environments is essential and would be planned in other future campaigns.

REFERENCES

De Backer, H., P. Koepke, A. Bais, X. de Cabo, T. Frei, D. Gillotay, C. Haite, A. Heikkilä, A. Kazantzidis, T. Koskela, E. Kyrö, B. Lapeta, J. Lorente, B. Mayer, H. Plets, A. Redondas, A. Renaud, A. Schmalwieser and K. Vanicek (2001): "Comparison of measured and modelled UV Indices for the assessment of health risks". *Meteorol. Appl.* **8**, 267-277.

Gueymard, C. (1995): "SMARTS2, A Simple model of the atmospheric radiative transfer of sunshine: algorithms and performance assessment". Florida Solar Energy Center, Rep. FSEC-PF-270-95, 83 pp. Florida.

Koepke, P., A. Bais, D. Balis, M. Buchwitz, H. De Backer, X. de Cabo, P. Eckert, P. Eriksen, D. Gillotay, T. Koskela, B. Lapeta, Z. Litynska, J. Lorente, B. Mayer, A. Renaud, A. Ruggaber, G. Schauberger, G. Seckmeyer, P. Seifert, A. Schmalweiser, H. Schwander, K. Vanicek and M. Weber (1998): "Comparison of models used for UV index-calculations". *Photochem. Photobiol.*, **67**, 6, 657-662.

Lorente, J., A. Redaño and X. de Cabo (1994): "Influence of urban aerosol on spectral solar irradiance". *J. Appl. Meteor.*, **33**, 406-415.

Mayer, B. and G. Seckmeyer (1997): "Systematic long-term comparison of spectral UV measurements and UVSPEC modelling results". *J. Atmos. Res.*, **102**, D7, 8755-67.

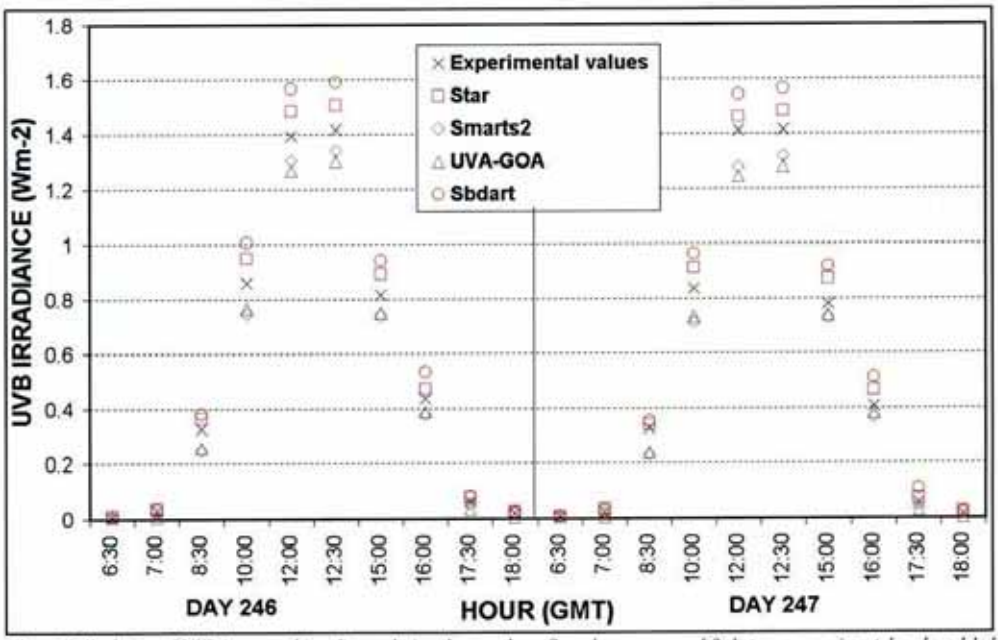

Figure 7. *Evolution of UVB integrated irradiance during the two days. One observes a good fit between experimental and modeled values. Here we observe a greater desviation near noon.*

McKinley, A. F. and B. L. Diffey (1987): "A reference action spectrum for ultraviolet induced erythema in human skin". *CIE J.* **6**, 17-22.

Ruggaber, A., R. Dlugi, and T. Nakajima (1994): "Modeling of radiation quantities and photolysis frequencies in the troposphere". *J. Atmosph. Chem.*, **18**, 171-210.

Schwander, H., P. Koepke and A. Ruggaber (1997): "Uncertainties in modelled UV irradiances due to limited accuracy and availability of input data", *J. Geophys. Res.*, **102**, D8, 9419-9429.

Webs, P. and A. R. Webb (1997): "Accuracy of spectral UV model calculations". Part I: Consideration of the uncertainties in the input parameters. *J. Geophys. Res.* **102**, 1551-1560.

C.4 Boletín del Grupo Español de Fotobiología, 2004; 22-26

XVIII Reunión Grupo Español de Fotobiología
Málaga, 20-21 de Febrero de 2004
22

Dosimetría comparada de la radiación UV solar y de lámparas UV de uso frecuente

Lorente, J.
de Cabo, X.
Campmany, E.
Sola, Y.

Departamento de Astronomía y Meteorología.
UNIVERSIDAD DE BARCELONA

1. Introducción y terminología

La radiación UV solar constituye aproximadamente el 5% de la radiación energética solar total que incide al nivel del suelo. A la porción UVB (280-320 nm), que suele representar menos del 0,5% de la radiación solar total, se le atribuye un conjunto de efectos negativos sobre la piel humana (eritema solar, daños en el ADN, inmunosupresión y, a largo plazo, cáncer cutáneo). La porción UVA (320-400 nm) puede causar también efectos negativos en la piel, algunos de los cuales se relacionan con la formación de productos de oxidación que dañan las células cutáneas [1] Generalmente el efecto eritemático de la radiación UV, ha servido como referencia para definir algunas magnitudes muy utilizadas en fotobiología y que podemos resumir aquí:

El espectro de acción, que indica la efectividad relativa de la radiación UV para producir eritema según su longitud de onda. Suele adoptarse el propuesto por la Comisión Internacional de Iluminación (CIE) también denominado espectro de acción Diffey [2] que se muestra en la figura 1 y que tiene su máximo en 298 nm. La enorme diferencia entre el efecto eritema de la radiación UVB y el correspondiente a la UVA, hace que con frecuencia solamente se considere la primera a efectos de fotoprotección.

La irradiancia biológicamente efectiva I_{be}, que constituye una medida biológica de la intensidad de la radiación UV y que se define como una media ponderada de la irradiancia UV espectral con el espectro de acción:

$$I_{be} = \int_{280}^{400} I_\lambda \, \varepsilon_\lambda \, d\lambda$$

donde I_λ y ε_λ son, respectivamente, la irradiancia y efectividad relativa para cada longitud de onda λ.

Dado que suele adoptarse $\varepsilon_{298\,nm} = 1$, la irradiancia biológicamente efectiva I_{be} es muy inferior a la correspondiente magnitud física de la irradiancia en el UVB. Representa, pues, el valor que tendría que tener una irradiancia monocromática de 298 nm para producir el mismo efecto que la irradiancia UV. Suele ser entre un 5% y un 10% de la irradiancia solar UVB. Así, en nuestras latitudes a mediodía en verano y con

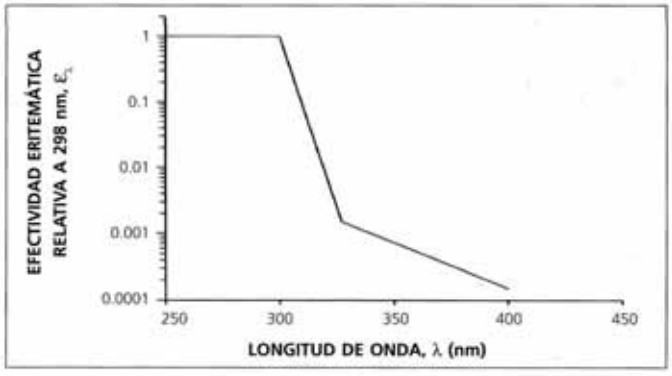

Figura 1. Espectro de acción CIE

Tabla I - Valores del índice UV solar e irradiancia asociada

UVI	GRADO	IRRADIANCIA BIOLÓGICA EFECTIVA (W/m^2))	DOSIS POR HORA (J/m^2)	MED II POR HORA
< 3	Bajo	< 0,075	< 270	~ 1
3-5	Moderado	0,075 - 0,138	270 - 495	1 – 2
6-7	Alto	0,138 – 0,187	495 - 675	2 – 3
8-10	Muy alto	0,187 - 0,262	675 - 943	3 - 4
>10	Extremo	> 0,262	> 943	> 4

cielos despejados, los valores típicos de la irradiancia solar UVB se sitúan en torno a 3-5 W/m^2 mientras que la irradiancia biológicamente efectiva es del orden de 0,2-0,3 W/m^2.

Índice UV (UVI), que se define como la irradiancia I_{be} multiplicada por 40. La tabla 1 muestra la clasificación del índice UV en grados de intensidad según la irradiancia biológicamente efectiva adoptada en la ACCIÓN COST 713 de la Unión Europea [3].

Las dosis eritemáticas mínimas (MED) asociadas a cada fototipo de piel. Representa el valor de la irradiación o dosis biológicamente efectiva necesaria para producir la reacción eritemática en cada uno de los tipos de piel. Según recomendaciones [3] de la Acción COST 713 de la UE, los valores de las MED corresponden a:

- ***Fototipo I:*** *200 J/m².*
- ***Fototipo II:*** *250 J/m².*
- ***Fototipo III:*** *350 J/m².*
- ***Fototipo IV:*** *450 J/m².*

Tiempos de exposición máximos para no sobrepasar la MED en cada fototipo suponiendo que la piel no está protegida frente a la radiación UV. Dicho tiempo se calcula dividiendo cada valor de la MED asociada a un fototipo por la irradiancia biológicamente efectiva I_{be} .

Factores de protección solar (SPF), de un fotoprotector que representa el factor por el que habría que multiplicar el tiempo de exposición a la radiación solar UV en una piel fotoprotegida con respecto a la piel sin esta protección para alcanzar la misma MED.

Estos mismos conceptos y terminología pueden aplicarse a las fuentes artificiales de luz UV. No obstante, al tener un espectro específico propio de cada lámpara, no serán aplicables los porcentajes entre radiación UV expresada en unidades físicas y la correspondiente biológicamente efectiva mencionados para la radiación solar.

2. Distribución espectral de la radiación emitida por lámparas UV

Las lámparas UV tienen un espectro muy variado, dependiendo del tipo de lámpara que se considere. La figura 2 muestra un ejemplo de comparación de los espectros de algunas de estas fuentes de luz UV en comparación con la distribución espectral de la radiación solar UV. Se incluye una muestra de 4 tipos de lámparas utilizadas en centros de bronceado, dos correspondientes a un simulador solar y las gráficas de los espectros de irradiancia solar UV de un día típico de verano en Barcelona y en el Pico Veleta (3398 m de altitud). En todas las gráficas se observa que el máximo de irradiancia UV tiene lugar en el UVA, pero existen marcadas diferencia en la irradiancia para las longitudes de onda más cortas (UVB). Como consecuencia, la irradiancia biológicamente efectiva varía notablemente de unas lámparas a otras, como se observa en la tabla que acompaña a la figura 2.

3. Espectro y dosis del simulador solar

El simulador solar presenta un espectro similar al solar en el intervalo UVB y UVA más corto (hasta unos 365 nm) pero con una intensidad regulable que puede llegar a ser mucho mayor que la irradiancia solar. La figura 3 muestra estos espectros comparados, en los que se han incluido dos distribuciones espectrales de la radiación solar multiplicadas por 16, una de ellas correspondiente al mediodía de un día de verano en Barcelona y otra correspondiente a un espectro al mediodía en el pico Veleta. El simulador solar corresponde a un modelo de la casa Solar Light.

Málaga, 20-21 de Febrero de 2004
XVIII Reunión Grupo Español de Fotobiología

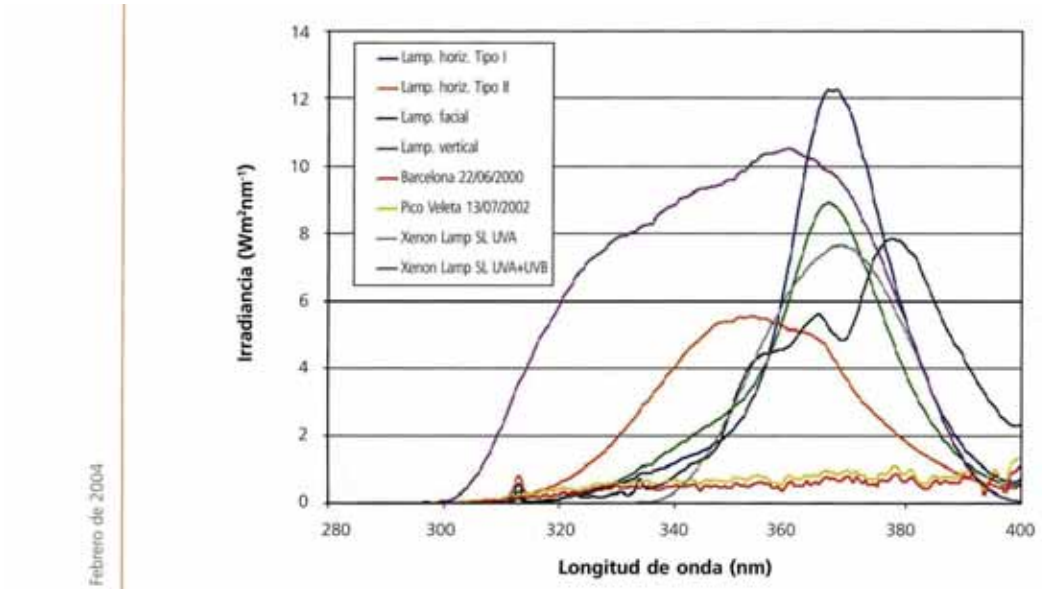

FUENTE DE LUZ	I_{UV}	I_{UVBe}	I_{UVB}	I_{UVBBe}	I_{UVA}	I_{UVABe}	UVI
Radiación solar *Barcelona*	46.6	0.165	1.38	0.135	45.2	0.030	6.6
Radiación solar *Veleta*	62.8	0.267	3.76	0.226	59.1	0.041	10.7
Simulador solar Solar Light *Canal UVA*	234	0.094	$2.28\ 10^{-3}$	$8.99\ 10^{-4}$	234	0.094	4
Simulador solar Solar Light *Canal UVA+UVB*	611	2.98	53.7	2.46	556	0.51	119
Lámpara bronceado *Horiz. Tipo I*	308.4	0.268	1.82	0.135	306.6	0.132	10.7
Lámpara bronceado *Horiz. Tipo II*	240.7	0.371	4.75	0.203	236.0	0.167	14.8
Lámpara bronceado *Facial*	276.5	0.143	0.76	0.037	275.7	0.106	5.7
Lámpara bronceado *Vertical*	253.1	0.204	1.42	0.085	251.7	0.121	8.2

Figura 2. Distribuciones espectrales de la radiación emitida por varios tipos de lámparas de bronceado, simulador solar y radiación solar en diferentes localizaciones (arriba). La tabla muestra los valores (en W/m²) de la irradiancia total I_{UV}, irradiancia biológicamente efectiva I_{UVBe} las correspondientes en los rangos espectrales UVA, UVB y el índice ultravioleta (UVI).

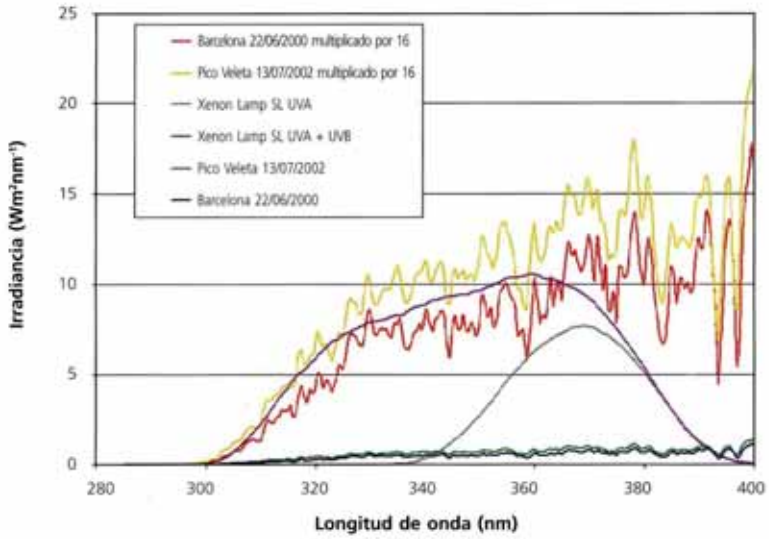

Figura 3. Espectro de un simulador del modelo Solar Light comparado con el de la radiación solar

La alta irradiancia UVB que puede proporcionar el simulador solar determina a su vez un UVI muy alto en comparación con los valores del UVI solar que se muestran en la tabla 1. En el modelo estudiado, el simulador alcanza un UVI máximo de 119, que corresponde a 43 MED II por hora, o lo que es lo mismo, una MED II cada 84 s. Para longitudes de onda próximas al visible la irradiancia que da el simulador es relativamente baja, inferior a la solar para longitudes de onda superiores a los 395 nm.

4. Espectro y dosis de las lámparas de bronceado

En las cabinas de bronceado podemos encontrar una extensa gama de tipos de fuentes de luz UV, cuyo estudio detallado no abordaremos aquí. Nos referiremos solamente a las medidas realizadas en algunas de las cabinas de bronceado más utilizadas en los centros dedicados a esta actividad. De los cuatro espectros analizados, tres de ellos son lámparas de baja presión de tipo tubos fluorescentes dispuestos en cabinas verticales y horizontales para irradiación corporal y uno es de alta presión con los filtros adecuados para su uso en irradiación facial. La figura 3 muestra estos espectros, incluyendo el de la radiación solar cuya comparación con las otras fuentes de luz analizadas aparece también en la figura 2.

Como aspectos significativos destacaremos la relativamente baja irradiancia UVB que producen estas lámparas, inferior a la UVB solar, mientras que su irradiancia UVA es muy alta en comparación a la recibida del Sol. Así, la "lámpara horizontal tipo I" tiene un máximo a 370 nm que es unas 14 veces superior a la solar recibida en verano al mediodía para esta longitud de onda y unas 6 veces superior a la media climatológica de irradiancia solar UVA medida en Barcelona [4].

La irradiancia biológicamente efectiva que emiten estas lámparas depende fundamentalmente de su proporción en UVB, pero también contribuye en proporción significativa la alta radiación UVA que emiten, sobre todo en las lámparas que tienen su máximo en longitudes de onda UVA más cortas. Este es el caso de la "lámpara horizontal tipo II" que, a pesar de tener una irradiancia UVA inferior a la de tipo I, el hecho de presentar su máximo a 350 nm en vez de tenerlo a 370 nm, determina un UVI superior, que alcanza un valor de 14,8. No obstante, hay que señalar que ambos tipos de lámparas tienen un UVI de grado extremo, con MED II que se alcanzan en 15 y 11 minutos respectivamente.

5. Normativa sobre dosimetría UV en centros de bronceado

El Real Decreto 1002/2002 [5] establece que los usuarios de aparatos de bronceado no podrán recibir radiaciones UV con una irradiancia efectiva, medida según Norma UNE EN 60 335-2-27, superior

XVIII Reunión Grupo Español de Fotobiología Málaga, 20-21 de Febrero de 2004

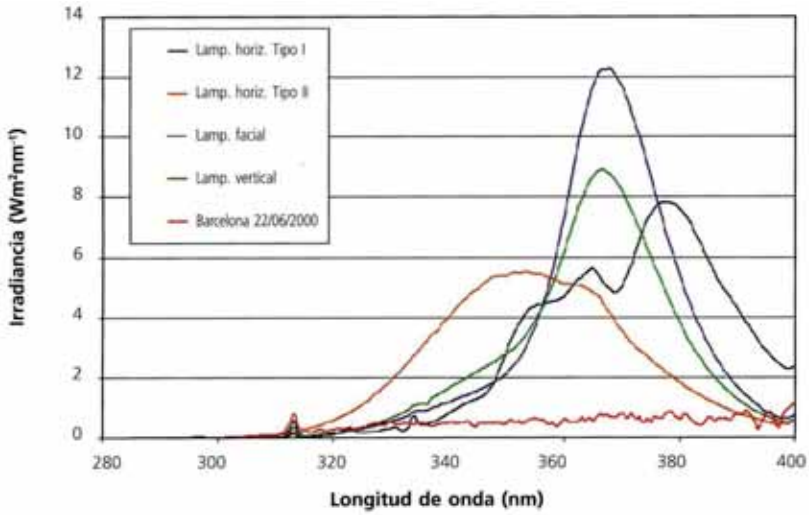

Figura 3. Comparación de los espectros UV medidos en 4 cabinas de bronceado

a los 0,30 W/m², ni tampoco recibir radiaciones con longitud de onda por debajo de los 295 nm. La irradiancia "efectiva" mencionada en el Decreto corresponde a la que aquí se ha denominado "biológicamente efectiva" y el valor máximo que se establece corresponde a un índice UVI = 12, valor que se considera extremo según la normativa europea mostrada en la tabla 1.

En una campaña inicial de medidas espectrorradiométricas realizada por nuestro grupo en diversos tipos de cabinas comerciales destinadas a bronceado por irradiación UV, se comprobó que la mayor parte de los equipos examinados irradiaba valores biológicamente efectivos cercanos, y en algún caso superiores, a los valores máximos permitidos por la normativa mencionada, si bien en casi ninguno de ellos se comprobó irradiancia por debajo de 295 nm.

6. Conclusiones

A pesar de su nombre, la distribución espectral de irradiancia en simuladores solares y lámparas UV de "sol artificial" utilizadas en equipos comerciales de bronceado es muy variada y en todas ellas profundamente diferentes de la distribución de la radiación solar, tanto por su intensidad como en la proporción relativa de los diversos intervalos de longitud de onda. La mayoría de lámparas denominadas UVA contienen una cierta proporción de UVB, en general pequeña, pero que determina su principal contribución a la irradiancia biológicamente efectiva. Su alto valor de irradiancia UVA, que supera el 500% de la correspondiente a la radiación solar y que no queda de manifiesto en la medida de la irradiancia biológicamente efectiva, debe tenerse en cuenta para la evaluación de otros efectos negativos de la radiación UVA sobre la piel.

Referencias

[1] *Morley, N., A. Curnow, L. Salter, S. Campbell, D. Gould: N-acetyl –l-cysteine prevents DNA damage by UVA, UVB and visible radiation in human fibroblasts.* J. Photochemistry and Photobiology B, ***72***, *55-60 (2003).*

[2] *Mc Kinlay, A.F., and B.L. Diffey: A reference action spectrum for ultra-violet induced erythema in human skin.* Human Exposure to UV Radiation : Risks and Regulations. *Elsevier Science, 83-87 (1987)*

[3] *COST-713 Action:* UV Index for the Public. *ISBN; 92-828-8142-3. Office for Official Publications of the European Communities. Luxembourg. (2000)*

[4] *Lorente, J. A. Redaño, X. de Cabo: Influence of urban aerosol on spectral solar irradiance.* J. Applied Meteorology, *33, 406-415 (1994)*

[5] *BOE 243 del 10 de octubre de 2002. 35771-74 (2002)*

C.5 3a Asamblea Hispano-Portuguesa de geodesia y geofísica. Proceedings, 2002; TOMO III, 1394-1396

PREDICCIÓN DIARIA DEL ÍNDICE UV A PARTIR DE LA COLUMNA DE OZONO OBSERVADA POR EL TOMS

DAILY FORECASTING OF UV INDEX FROM OZONE OBSERVED BY TOMS

Lorente J., X. de Cabo, E. Campmany
Dep. d'Astronomia i Meteorologia, Universitat de Barcelona, Diagonal 647 080, Barcelona, jeroni@am.ub.es

SUMMARY

Forecasting of UV index (UVI) is nowadays an important issue to be made by some Meteorological Weather Services. The accurate multiple scattering models to be applied to obtain the UV-B solar radiation reaching the earth's surface need as input the forecast atmospheric transparency conditions, mainly the total column ozone, cloudiness and aerosol depth. Because of the ozone field forecasts are difficult to have in real time for most sites, a persistence hypothesis has been sometimes employed, based in the small day-to-day variations of the ozone layer during the summer in mid-latitudes. In this work we try to check the uncertainty in the forecast UVI for Barcelona by applying this hypothesis during the summer and spring seasons. Results show relative errors near to 6% in the UVI predicted during the summer. Taking into account the fact that UVI has values near 8 or 9 in this season, the forecast value, expressed as an integer value, is the same as the corresponding obtained with a more accurate algorithm for the ozone forecasting.

1. INTRODUCCIÓN

Desde el verano de 2000 en Cataluña se lleva a cabo la predicción diaria del índice ultravioleta (UVI), y se difunde al público junto con cierta información y recomendaciones sobre los tiempos máximos de exposición a la radiación solar y las medidas de protección a adoptar en función del tipo de piel individual. El UVI es un índice propuesto por la Organización Meteorológica Mundial, la Organización Mundial de la Salud y otras instituciones para representar de una manera sencilla el potencial efecto perjudicial de la radiación solar UV sobre la piel humana. El UVI se calcula multiplicando por 40 la iradiancia biológicamente efectiva, definida como la integral de la irradiancia espectral ponderada mediante el espectro de acción de referencia según McKinley y Diffey (1987).

Algunos trabajos realizados en la acción COS 713 de la Unión Europea Koepke et al. (1998) muestran la idoneidad de los modelos de dispersión múltiple para la predicción del UVI. El modelo SBDART (Santa Barbara DISORT Atmospheric Radiative Transfer), Ricchiazzi et al. (1998) es uno de ellos y se ha aplicado en la predicción del UVI para Cataluña. Dado que inicialmente no se disponía de un algoritmo adecuado para la predicción de ozono, en la campaña de predicción diaria de este índice se utilizó el dato de ozono más reciente disponible, aplicando la hipótesis de persistencia en la columna de ozono, cuya variación en verano no suele exceder del 1% (Long et al., 1996). El presente trabajo analiza los resultados de las predicciones adoptando esta hipótesis.

2. DATOS Y METODOLOGÍA

Las medidas de ozono que se han utilizado para realizar este trabajo son las proporcionadas por los sensores TOMS (Total Ozone Mapping Spectrometer), a bordo de los satélites Earth Probe de la NASA. Las medidas de irradiancia eritemática estudiadas han sido obtenidas con un espectroradiómetro Bentham DMc300 de doble monocromador instalado en la terraza de nuestro Departamento de Astronomía y Meteorología (41.35 N, 2.17 E).

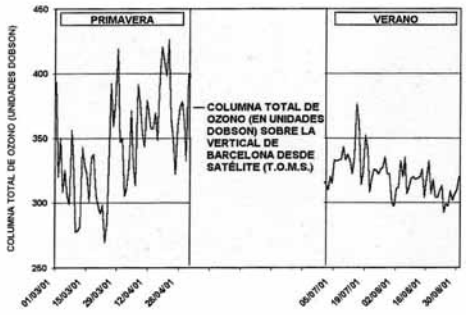

Figura 1 **- Variación de la columna total de ozono en primavera y verano.** ***(Variation of the ozone in spring and summer .).***

Para caracterizar las diferencias entre primavera y verano se han elegido los meses de marzo, abril, julio y agosto del año 2001. En total se han estudiado 123 días de los cuales se ha considerado sólo los días con condiciones de cielo despejado durante el mediodía (100 días).

Para cada día se ha ejecutado tres veces el modelo SBDART con el ozono del mismo día, el ozono del día anterior y el ozono de dos días anteriores. En la figura 2 se compara la predicción de la irradiancia eritemática utilizando el valor de la columna total de ozono del día correspondiente con la medida realizada con el espectroradiómetro.

C.5. 3a Asamblea Hispano-Portuguesa de geodesia y geofísica. Proceedings, 2002; TOMO III, 1394-1396

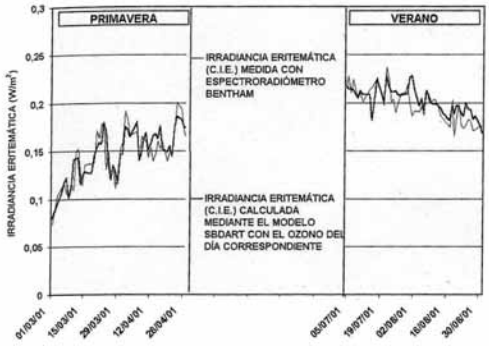

Figura 2 - **Comparación entre la irradiancia eritemática medida y la modelizada .** ***(Comparision between measured irradiance and modeled).***

3. RESULTADOS

Para evaluar la bondad de las distíntas prediciones se han calculado los errores relativos en porcentaje (tabla 1, figura 3 y figura 4) así como el error cuadrático medio (tabla 2 y figura 5). Observando los resultados se puede concluir que la hipótesis de persistencia de la columna total de ozono es valida en verano, incluso para 2 días, pero no en primavera.

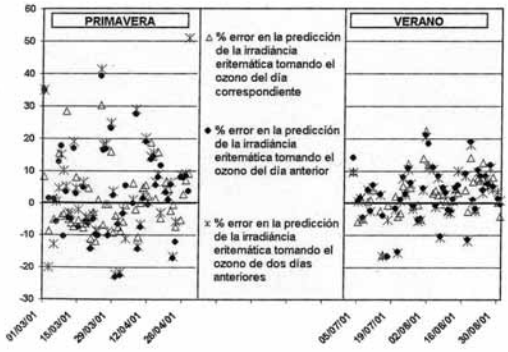

Figura 3 - **Errores relativos entre las 3 previsiones y las medidas de la irradiancia eritemática.** ***(Relative errors between the 3 forecasts and the measured irradiance).***

Tabla 1 - Promedio de los errores relativos en la predición de la irradiancia eritemática (*Mean of relative errors in eritemathic irradiance forecast*)

Input	Primavera	Verano
Ozono del día correspondiente	7,23 %	5,15 %
Ozono del día anterior	10,47 %	6,30 %
Ozono de 2 días anteriores	11,43 %	6,12 %

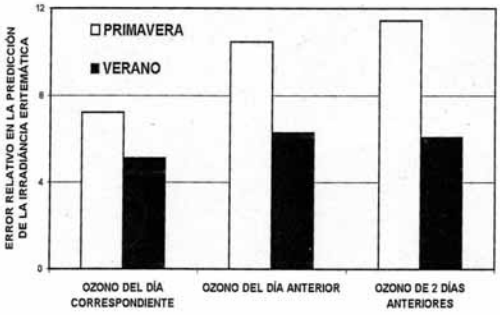

Figura 4 – **Promedio de los errores relativos en la predicción de la irradiancia eritemática.** ***(Mean of the relative errors in eritemathic irradiance forecast.).***

Tabla 2 - Error cuadrático medio en la predición de la irradiancia eritemática *(Mean square error in eritemathic irradiance forecast)*

Input	Primavera	Verano
Ozono del día correspondiente	1,32 E-2 W/m²	1,33 E-2 W/m²
Ozono del día anterior	1,89 E-2 W/m²	1,60 E-2 W/m²
Ozono de 2 días anteriores	2,21 E-2 W/m²	1,51 E-2 W/m²

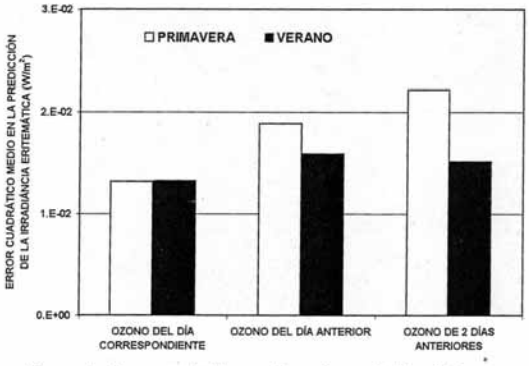

Figura 5 - **Error cuadrático medio en la predicción de la irradiancia eritemática.** ***(Mean square error in eritemathic irradiance forecast.).***

4. CONCLUSIONES

La hipótesis de persistencia es una herramienta útil para la previsión del UVI en verano siendo válida incluso para 2 días. Los resultados obtenidos muestran ajustes con un error relativo alrededor del 6%. La repercusión en los valores del UVI, teniendo en cuenta que en verano se alcanzan valores alrededor de 8 o 9, es menor que media unidad. Esto implica que la predicción del índice ultravioleta, debido a que se expresa con una sola cifra significativa, generalmente difiere en menos de una unidad que cuando se realiza con algoritmos más precisos para la predicción de ozono.

5. REFERENCIAS

- Lorente J., Redaño A. y de Cabo X., (1994): "Influence of urban aerosol on spectral solar irradiance". *Journal of Applied Meteorology* **33**, 406-415.
- Cooperation in Science and Technology. COST-713 action (UV-B Forecasting)
- Long C. S., Miller A.J., Lee J.T., Wild J.D., Pryzywarty R.C. y Hufford D., (1996): "Ultraviolet index forecasts issued by the National Weather Service". *Bulletin American Meteorolgy Society*, **77**, 729-748.
- McKinley A.F. y Diffey B.L., (1987): "A reference spectrum for ultraviolet induced erythema in human skin". *CIE Journal*, **6** , 1.
- Koepke, P., Bais, A., Balis, D., Buchwitz, M., De Backer, H., de Cabo, X., Eckert, P., Eriksen, P., Gillotay, D., Koskela, T., Lapeta, B., Litynska, Z., Lorente, J., Mayer, B., Renaud, A., Ruggaber, A., Schauberger, G., Seckmeyer, G., Seifert, P., Schmalwieser, A., Schwander, H., Vanicek, K. y M. Weber (1998): "Comparision of models used for UV Index calculations". *Photochemistry and Photobiology* **67**(6): 657-662.
- Ricchiazzi, P.J., S. Yang, and C. Gautier, (1998): "SBDART: A research and teaching software tool for plane-parallel radiative transfer in the Earth's atmosphere", *Bulletin of the American Meteorological Society*, **79**, 2101-2114

6. AGRADECIMIENTOS

Este trabajo se ha realizado en el marco del proyecto REN2000-0903-C08CLI